

An Optical View of BL Lacertae Objects

Renato Falomo · Elena Pian
· Aldo Treves

Received: date / Accepted: date

Abstract BL Lac objects are active nuclei, hosted in massive elliptical galaxies, the emission of which is dominated by a relativistic jet closely aligned with the line of sight. This implies the existence of a parent population of sources with a misaligned jet, that have been identified with low-power radiogalaxies. The spectrum of BL Lacs, dominated by non-thermal emission over the whole electromagnetic range, together with bright compact radio cores, high luminosities, rapid and large amplitude flux variability at all frequencies and strong polarization make these sources an optimal laboratory for high energy astrophysics. A most distinctive characteristic of the class is the weakness or absence of spectral lines, that historically hindered the identification of their nature and ever thereafter proved to be a hurdle in the determination of their distance. In this paper we review the main observational facts that contribute to the present basic interpretation of this class of active galaxies. We overview the history of the BL Lac objects research field and their population as it emerged from multi-wavelength surveys. The properties of the flux variability and polarization, compared with those at radio, X-ray and gamma-ray frequencies, are summarized together with the present knowledge of the host galaxies, their environments, and central black hole masses. We focus this review on the optical observations, that played a crucial role in the early phase of BL

Renato Falomo
INAF-Osservatorio Astronomico di Padova, Vicolo dell'Osservatorio 5, 35122 Padova, Italy
Tel.: +39-049-8293464
Fax: +39-049-8759840
E-mail: renato.falomo@oapd.inaf.it

Elena Pian
INAF-Istituto di Astrofisica Spaziale e Fisica Cosmica, Via P. Gobetti 101, 40129 Bologna, Italy; Scuola Normale Superiore, Piazza dei Cavalieri 7, 56126 Pisa, Italy; INFN, Sezione di Pisa, Italy

Aldo Treves
Università dell'Insubria, Via Valleggio 11, 22100 Como, Italy; INFN, Sezione di Milano Bicocca, Italy; ICRA

Lacs studies, and, in spite of extensive radio, X-ray, and recently gamma-ray observations, could represent the future major contribution to the unveiling of the origin of these sources. In particular they could provide a firm conclusion on the long debated issue of the cosmic evolution of this class of active galactic nuclei and on the connection between formation of supermassive black holes and relativistic jets.

Keywords Galaxies: active · Galaxies: nuclei · Galaxies: jets · BL Lacertae objects: general · quasars: supermassive black holes · Radiation mechanisms: non-thermal

Preface

Discovered and classified as an irregularly variable star by Hoffmeister (1929), BL Lacertae was found to have a radio counterpart (MacLeod & Andrew, 1968). This, together with the high optical polarization, drew attention on this source and on others that exhibited similar properties, primarily a highly variable and featureless, power-law-shaped optical spectral continuum. This class of objects was soon recognized to be extragalactic in nature and to share some of the characteristics of quasars (Strittmatter et al., 1972). Supporting evidence of this came from the detection of a surrounding nebulosity centered on the optical point-like source (first noted by Schmitt, 1968), that hinted at the presence of a host galaxy (Ulrich, 1978, 1989).

The peculiarities that make BL Lac objects (BLLs) so enigmatic can be composed in a coherent picture that foresees a relativistic jet viewed at a small angle as the main responsible of all multi-wavelength BLL characteristics (Blandford & Rees, 1978). This explanation was later reinforced by the elaboration of a unifying scenario that envisages radiogalaxies, for which kiloparsec-scale jets are directly observed, and BLLs as members of the same population, with the viewing angle determining the different observed properties.

Thanks to their widely extended spectral energy distribution, that covers sixteen decades in frequency, from the radio to TeV, BLLs can be detected with observations at any frequency. In fact, surveys at radio, optical, X-ray and gamma-ray frequencies in the last 40 years have contributed to select BLL candidates. After identification via optical spectroscopy, samples of bona fide BLLs have been constructed at different frequencies and have made the statistical study of the population possible. A crucial parameter for assessing their cosmological role and evolution is their redshift, a quantity that is intrinsically difficult to determine in BLLs and for which accurate optical spectroscopy is critical. By 1976 there were 30 known BLLs (Stein et al., 1976); almost forty years on, there are nearly 1400 catalogued BLLs (Véron-Cetty & Véron, 2010).

Notwithstanding the importance of the multi-wavelength investigation, the observation and analysis of BLLs in the optical band remain a mainstay of research in this field, as witnessed by the advances in the last decade. In this review we have therefore focused on the optical domain. The first specific

review on BLLs was that of Stein et al. (1976). BLLs were the subject of three dedicated conferences: at the University of Pittsburgh in 1978 (Pittsburgh Conference on BL Lac Objects, Proceedings edited by A.M. Wolfe, NSFP Pittsburgh, 1978), in Como, Italy, in 1988 (BL Lac Objects, Eds. L. Maraschi, T. Maccacaro, M.-H. Ulrich, Lecture Notes in Physics, Springer-Verlag, 1989), and in Turku, Finland, in 1998 (BL Lac phenomenon, Eds. L. O. Takalo and A. Sillanpää, Astronomical Society of the Pacific, 1999).

1 Introduction

Galaxies are traditionally divided in active and inactive, according to whether their nuclei exhibit the telltale signs (broad emission lines, flux variability, radio compactness, strong emission at high energies) of a central “engine” or not. However, the distinction is not sharp and there is a continuum of properties between these two extremes, with a wide range of nuclear activity levels, that accordingly define different types of active galactic nuclei (AGNs). The most powerful among these are luminous emitters over the whole electromagnetic spectrum up to the TeV energies, highly variable and highly polarized (bolometric luminosities can reach 10^{48} erg s $^{-1}$ and are often dominated, especially during outbursts, by the gamma-ray emission). These are called “blazars”¹.

There is unanimous consensus on the fact that blazars owe their extreme physical behavior to the presence of a jet that is closely aligned with the observer’s direction (estimated viewing angles $\theta \lesssim 10$ deg) where the plasma moves with a Lorentz² factor Γ of the order of ~ 10 , and occasionally as high as ~ 50 (Begelman et al., 2008). The highly relativistic kinematic regime and the small viewing angle produce a Doppler aberration (quantified by the factor $\delta = [\Gamma(1 - \beta \cos\theta)]^{-1}$), that foreshortens the observed time-scales, blue-shifts the observed spectrum and magnifies³ the luminosities at all wavelengths (e.g. Ghisellini et al., 1993; Urry & Padovani, 1995; Ghisellini, 2013). Direct evidence for this interpretation comes from the detection of superluminal motion of plasma blobs along the jet, the apparent velocity of which, as measured with radio interferometry, can be up to $20c$ (Marscher et al., 2008; Jorstad et al., 2010).

When corrected for Doppler aberration, these velocities are obviously lower than the speed of light, and compatible with a Lorentz factor of the order of 10. Indirect arguments for relativistic beaming include: i) the super-Eddington accretion regimes for putative central black hole masses of $\sim 10^8 M_{\odot}$; ii) the transparency of the emitting regions to electron-positron pair-production at gamma-ray energies higher than ~ 1 MeV (McBreen, 1979; Guilbert et al., 1983; Maraschi et al., 1992); iii) the huge radio brightness temperatures. If

¹ This term was coined by E. Spiegel during the Conference on BL Lac Objects in Pittsburgh, in April 1978, from a contraction of “BL Lac” and “quasar”.

² Γ is defined as $(1 - \beta^2)^{-0.5}$, where $\beta = v/c$, with v representing the plasma velocity.

³ In general the luminosity enhancement is a factor δ^p , where $3 \lesssim p \lesssim 4$, depending on the geometry of the emitting region and on spectral index.

no beaming is invoked then one would expect self-absorbed radio spectra over wide radio wavelength ranges and the Compton catastrophe in the X-rays. None of these effects are observed (Hoyle et al., 1966; Woltjer, 1966; Kellermann & Pauliny-Toth, 1969).

The interpretation of the blazar class as relativistically beamed objects implies the existence of a parent population of misaligned sources. Based on optical and radio properties and population density, the most favored candidates are radiogalaxies⁴ that would be detected and classified as blazars when viewed at small angles (Urry & Padovani, 1995).

The term *blazar* encompasses bright radio-loud AGNs with compact radio cores, high amplitude multi-wavelength variability and large radio and optical polarization. Historically, those with weak or absent optical spectral lines were named BL Lac objects (see also Section 6), and the others received definitions that reflected their main properties: Optically Violently Variables, or Highly Polarized Quasars (e.g., Moore & Stockman, 1981). More recently, the distinction within the blazar class was drawn between objects with luminous broad emission lines, often accompanied also by prominent ultraviolet-optical continuum emission (*blue bump*) of thermal origin as normally seen in quasars, that are called Flat Spectrum Radio Quasars (FSRQ) and BLLs, where these broad emission lines are weak or absent (Urry & Padovani, 1995; Padovani et al., 2012). This distinction is reflected also in the radio polarization properties: at cm wavelengths BLLs tend to have polarization vectors nearly parallel to the jet, while in FSRQs the vectors cover a wider range of directions, favoring directions perpendicular to the jet (Gabuzda et al., 1989; Marscher et al., 2002). Owing to these different properties, and in particular to the lack of a substantial thermal component (accretion disk and/or dusty torus), BLLs offer a more direct view into the primary energy-production mechanism, with respect to FSRQs.

This review is organized as follows: in Section 2 we present the basic multi-wavelength properties and the reference model for BLLs; Section 3 reviews the methods of detection and selection of BLLs through surveys and the luminosity functions; Section 4 reports on the optical, near-infrared and ultraviolet variability of BLLs; Section 5 summarizes the optical polarization issues; the optical spectral properties, both from broad-band photometry and spectroscopy, are described in Section 6; the observations of host galaxies are reviewed in Section 7; a few BLL sources exhibited optical counterparts to their radio jets, as detailed in Section 8; the close environments and clustering properties of BLLs are reported in Section 9; Section 10 focuses on the central supermassive black hole, on its influence on the observed properties and on its mass measurement. Section 11 contains a summary and future perspectives.

⁴ Fanaroff & Riley (1974) distinguished radiogalaxies into two types: FR I and FR II according to whether their luminosities at 178 MHz were lower or higher than 2×10^{32} erg s⁻¹ Hz⁻¹sr⁻¹. Their radio morphologies are also different, being core-dominated or lobe-dominated, respectively. The comparison of radio power and morphology and host galaxy luminosity of BLLs and radiogalaxies suggests that the dominant parent population consists of FR I radiogalaxies.

2 Multi-wavelength properties and the reference model

BLLs are characterized by strong non-thermal emission at all frequencies. In the radio band, they exhibit bright (up to 10^{31} erg s $^{-1}$ Hz $^{-1}$, Padovani et al., 2007), compact cores with power-law spectral continua with very flat shapes ($F_\nu \propto \nu^{-\alpha}$ with $\alpha < 0.5$), mostly produced by synchrotron radiation, often partially self-absorbed at the GHz frequencies⁵.

At infrared-optical wavelengths the spectrum of BLLs also follows a power-law, when corrected for Galactic extinction and host galaxy contribution. The optical/near-infrared spectral indices are in the range $\alpha_\nu \sim 0.5 - 1.5$, i.e. they are steeper than in the radio (Falomo et al., 1993a,d; Pian et al., 1994). If the radio-to-optical spectrum is produced by the same optically thin synchrotron radiation component, the spectral steepening between these bands is naturally expected by increasing synchrotron losses at higher frequencies and adiabatic expansion of the jet plasma. The precise spectral slopes and their variability are also regulated by acceleration mechanisms and time-scales (Kirk et al., 1998; Asano et al., 2014).

In the X-rays BLLs are powerful sources ($L_{1keV} \sim 10^{28}$ erg s $^{-1}$ Hz $^{-1}$), and in fact they were detected by many satellites in the last 40 years (Perlman et al., 1996; Sambruna et al., 1996; Wolter et al., 1998; Pian et al., 1998; Giommi et al., 1999; Maselli et al., 2010). The X-ray spectra are generally well described by single power-laws or curved slopes, depending on the emission mechanism. If this is synchrotron radiation, X-rays are generated by the highest energy electrons, so that the spectrum has a relatively steep spectral index ($\alpha_\nu \sim 1.3$). If the cooling frequency (or break frequency) of the synchrotron spectrum is located in the X-ray range, the spectrum has a convex shape in this band. On the other hand, in a leptonic jet scenario (which we favour with respect to the hadronic one, see below), X-rays may be due to Compton up-scattering of lower energy photons by the same electrons that produce the synchrotron spectrum (synchrotron self-Compton), so that the X-ray spectral shape is flat ($\alpha_\nu < 1$). In BLLs where the synchrotron component peaks below the X-ray range, the X-ray spectrum is occasionally concave and joins smoothly with the high energy tail of the observed synchrotron spectrum.

The observations conducted in the MeV-GeV range from satellites (first the *Compton* Gamma-Ray Observatory in 1991-2000 and recently the orbiting *Fermi* Gamma-ray Satellite and *AGILE*) detected large numbers (~ 1000 to date) of extra-galactic sources that turned out to be blazars, with very few exceptions (Hartman et al., 1999; Ackermann et al., 2011; Vercellone et al., 2011). A large subset of them are BLLs. The integrated luminosities in the range 0.1-10 GeV can reach 10^{49} erg s $^{-1}$.

Very high energy photons (> 100 GeV) from blazars were detected from the ground by atmospheric Cherenkov radiation telescopes starting about 20 years ago (Punch et al., 1992). About 50 TeV blazars are now known (see

⁵ The overlap of several spatial emission components may also make the radio spectrum deviate from a Rayleigh-Jeans shape, so that it appears thin, although the individual components may be self-absorbed.

e.g. Persic & de Angelis, 2008; Acciari et al., 2011; Aliu et al., 2011, 2013; Aleksić et al., 2011, 2012; H.E.S.S. Collaboration et al., 2013; Şentürk et al., 2013), many of which have redshift higher than ~ 0.2 . A substantial fraction of these⁶ are BLLs, especially of high-frequency-peaked type, in which TeV detection is favoured by the broad-band spectral shape (see below). At $z \sim 1$ the extragalactic infrared background suppresses the TeV flux via pair production, so that detection beyond this redshift is virtually impossible. The highest observed luminosities at energies larger than 100 GeV are $\sim 10^{46}$ erg s^{-1} (MAGIC Collaboration et al., 2008).

The gamma-ray emission dominates the spectral energy distribution of blazars in general, and BLL in particular, especially during flaring states, and is highly variable (down to sub-hour time-scales, Aharonian et al., 2009). In the leptonic scenario, this is ascribed to inverse Compton scattering of lower energy photons off the most relativistic electrons. Therefore the gamma-ray spectral shape is determined by the high energy tail of the electron distribution and by the shape of the spectrum of the scattered photons, which can be either optical-to-soft-X-ray synchrotron photons (synchrotron self-Compton) or photons external to the jet, like those from the accretion disk, broad-line region, dust torus (external Compton).

In Figure 1 we report an example of an overall spectrum of BLL. The spectral energy distribution has two humps, one peaking at the characteristic synchrotron cooling frequency (typically between the far-infrared and soft X-rays), and a second one attributed to inverse Compton cooling in the MeV-GeV range. These frequencies vary from object to object in a correlated way: to a larger frequency of the first hump corresponds a larger frequency of the second hump. Accordingly, BLLs – depending on their spectral energy distribution – were traditionally divided in low-frequency-peaked objects (LBLs) and high-frequency-peaked objects (HBLs, Padovani & Giommi, 1995). Objects with intermediate properties are called intermediate BLLs (IBLs). This distinction reflects broadly the previous concept of blazar classification according to radio or X-ray selection. The characteristic spectral maxima in fact favor naturally the detection of a given blazar in a specific band. More extended multi-wavelength observations on large datasets led to a more complex picture (see Section 3).

In Figure 2 we show spectral energy distributions of representative blazar sources. While the double-humped shape is present in all of them, the frequencies of the spectral peaks and their relative intensities differ significantly. Fossati et al. (1998) found that the spectral energy distribution shapes define a continuum of properties, whereby (i) the first peak occurs in different frequency ranges for different samples/luminosity classes, with most luminous sources peaking at lower frequencies; (ii) the peak frequency of the gamma-ray component correlates with the peak frequency of the lower energy one; (iii) the luminosity ratio between the high and low frequency components increases with bolometric luminosity (Fig. 2). In this picture, called *blazar*

⁶ see list at <http://tevcat.uchicago.edu>

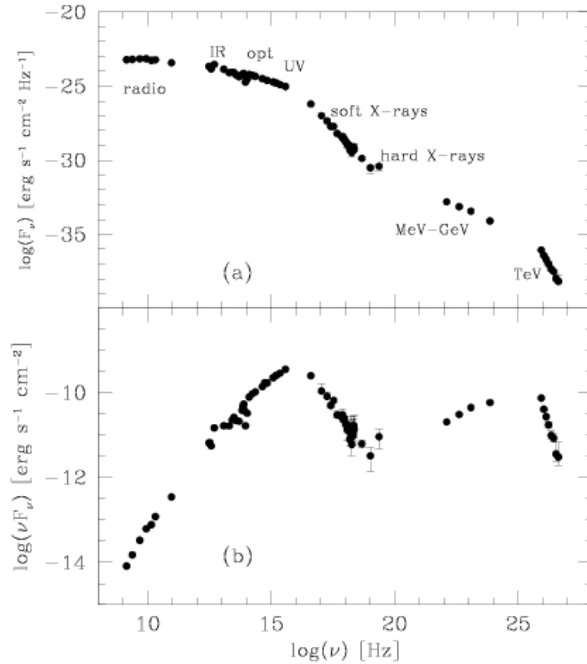


Fig. 1 Broad-band spectrum of PKS 2155–304 ($z = 0.116$). Panel (a): spectral flux distribution from radio to TeV frequencies; panel (b): νF_ν representation of the spectrum, that emphasizes the frequencies at which most of the power is emitted. Adapted from Foschini et al. (2007); H.E.S.S. Collaboration et al. (2012).

sequence, BLLs are the sources with lower luminosities and higher characteristic synchrotron and inverse Compton frequencies. The interpretation of this sequence is complex and somewhat controversial. The parameters that govern it are the cooling efficiency of the relativistic particles, the accretion efficiency and ultimately the mass of the central black hole, BLLs being those with lower efficiencies and lower masses (Costamante et al., 2001; Ghisellini & Tavecchio, 2008; Ghisellini et al., 2010). A number of objects deviate at first glance from this scheme, having comparatively high total luminosities and high synchrotron peak frequencies (Padovani et al., 2012; Potter & Cotter, 2013).

The central engine that powers the relativistic jet is assumed to be a rotating accreting black hole of about $10^8 M_\odot$. The mechanism of energy extraction and particle acceleration along the jet is however not completely understood (see e.g. Blandford & Znajek, 1977; Begelman et al., 1984; Maraschi & Tavecchio, 2003). The dynamics of the jet may be rather complex and it has in some cases been interpreted in terms of helical structures tightly related to the black

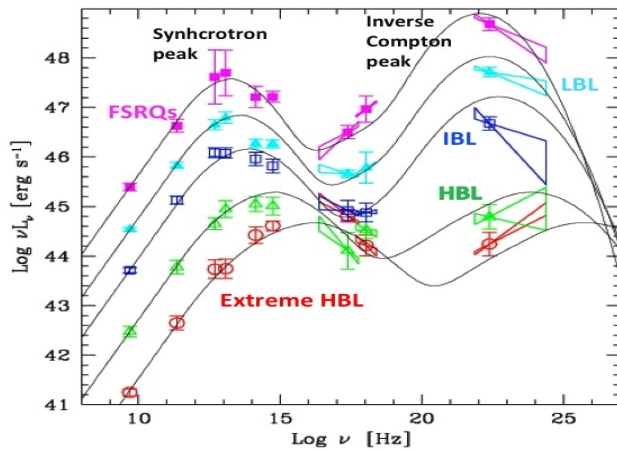


Fig. 2 Overall spectral energy distributions of blazars. Note the differences of the relative intensities and frequencies of the two emission peaks for various types of objects (see text). This behavior is referred to as blazar sequence (from Fossati et al., 1998).

hole spin or to the orbital motion of a binary black hole system (Camenzind & Krockenberger, 1992; Ostorero et al., 2004). On sub-parsec scales, jets are pervaded by magnetic fields of the order of 0.1-10 Gauss that may have tangled geometries and cause particles – leptons or hadrons – to radiate through the synchrotron mechanism.

As seen above, in the leptonic scenario the main emission mechanisms are synchrotron radiation of relativistic electrons at the radio to X-ray wavelengths, which is responsible for the first hump of the spectral energy distribution, and Compton up-scattering of synchrotron photons (self-Compton) or photon fields external to the jet at the higher energies, responsible for the second hump (Ghisellini et al., 1985, 1998; Błażejowski et al., 2000; Finke et al., 2008; Potter & Cotter, 2013). For self-Compton scattering (that is the most common case in BLLs), Klein-Nishina suppression (Moderski et al., 2005) may reduce the luminosity of the second hump and decrease its peak frequency.

In hadronic models, both primary electrons and protons are accelerated to ultrarelativistic energies, with protons exceeding the threshold for photo-pion production on the soft photon field in the emission region. While the low-frequency emission is still due to synchrotron emission from primary electrons, the high-energy emission is dominated by proton synchrotron emission, neutral pion decay photons, synchrotron and Compton emission from secondary decay products of charged pions, and the output from pair cascades initiated by these high-energy emissions intrinsically absorbed by photon-photon pair production (Mannheim & Biermann, 1992; Mannheim, 1998; Aharonian, 2000; Mücke & Protheroe, 2001; Mücke et al., 2003; Böttcher et al., 2013).

3 Demographics of BL Lacs

In order to understand the cosmological evolution of BLLs in comparison with other AGN and derive the properties of the unbeamed parent population it is mandatory to construct statistically significant samples of sources with measured redshift. Statistical samples are ultimately extracted from unbiased surveys carried out at various wavelengths. Depending on the adopted band, objects identified as BLL candidates, and then confirmed through the essential criterion of optical spectroscopy, are reported usually as radio, X-ray, optically, and also gamma-ray-selected objects (see Section 2). The characteristic double-peaked spectral energy distribution of BLLs (see Fig. 2) emphasizes the effects of single band flux-limited surveys. As an example, radio surveys preferentially select the sources with a low-frequency-peaked synchrotron component. On the other hand, in GeV surveys the objects with high-frequency inverse Compton component are favoured.

3.1 Surveys

The first complete flux-limited radio-selected sample of BLLs was constructed from the 1 Jy catalogue of radio sources of Kühr et al. (1981) containing 518 sources with $S_\nu > 1$ Jy at 5 GHz. The selection of BLLs from this catalogue was performed according to various properties (flat or inverted radio spectrum, optical magnitude and presence of weak spectral lines). This selection produced a list of 34 radio-selected BLLs (Stickel et al., 1991). The number counts derived from this sample (see Fig. 3, left) showed a roughly Euclidean behavior (no evolution), a result that was then later confirmed by more extended and complete studies (e.g. Caccianiga et al., 2008, and references therein).

Deep and systematic surveys undertaken in the 80's with the then orbiting X-ray satellites discovered BLLs and thus contributed to the construction of complete samples of BLLs selected on the basis of their X-ray emission. From the Extended Medium Sensitivity Survey of the *Einstein* X-ray satellite (0.3–3.5 keV, sensitivity $\sim 5 \times 10^{-14}$ erg s $^{-1}$ cm $^{-2}$, Gioia et al., 1990) Stocke et al. (1990) extracted a sample of 22 X-ray-selected BLLs. The *Einstein* Slew survey (Elvis et al., 1992) covered a much larger fraction of the sky with shallower sensitivity ($\sim 5 \times 10^{-12}$ erg s $^{-1}$ cm $^{-2}$). A result of this survey is a sample of 48 BLLs (Perlman et al., 1996). Further X-ray surveys with *ROSAT* and *Swift* allowed the discovery of about 100 new BLLs (Voges et al., 1999; Laurent-Muehleisen et al., 1998, 1999; Cusumano et al., 2010).

In the optical band the selection of BLLs is more tricky. The first BLLs discovered in the optical were derived from the search of ultraviolet excess stellar objects in the Palomar plates (Green et al., 1986). This resulted in the discovery of 7 objects (Fleming et al., 1993). Most fruitful recent optical searches of BLLs resulted from the analysis of pure optical spectra of SDSS sources. Plotkin et al. (2010), starting from the 7th SDSS spectroscopic data base (Abazajian et al., 2009) present a sample of ~ 700 BLL optically selected

candidates. A large fraction of the objects in the survey are of unknown redshift. Search for radio counterparts of these candidates showed that $\sim 90\%$ of these are radio-loud.

Owing to the blazar spectral energy distribution, that extends to very high energies, surveys in the GeV band turned out to be extremely efficient in finding BLLs, thanks to their regular and uniform sky coverage. In the 2nd Fermi LAT AGN Catalog (Ackermann et al., 2011), which contains ~ 1000 sources, 80% are blazars, of which about half are BLLs. The majority of the remaining 20% are blazar candidates. In the selection of candidates, near-infrared observations from the ground have been used in the past (see e.g. Bersanelli et al., 1992; Chen et al., 2005), but particularly effective were proven to be the spectra obtained from satellites (e.g. *Spitzer*, Chen & Shan, 2011), and especially the infrared colors from *WISE* observations, because gamma-ray blazars detected by *Fermi* occupy a distinctive strip in the 3.4-4.6, 4.6-12 μm color-color diagram (Massaro et al., 2012a, 2013; D'Abrusco et al., 2013; Paggi et al., 2013). These candidates must be eventually confirmed via optical spectroscopy.

At variance with most AGNs, since BLLs are strong emitters at any wavelength, they can be detected in surveys performed in various spectral bands. Moreover, owing to the high-amplitude flux variability they may appear in a survey depending on their activity state. Modern BLL catalogs are based on multi-wavelength data and reflect more accurately the full range of their spectral and timing properties (Schwartz & Ku, 1983; Perlman et al., 1996; Maccacaro et al., 1998; Giommi et al., 1999; Beckmann et al., 2003; Giommi et al., 2005; Padovani et al., 2007; Massaro, E. et al., 2009).

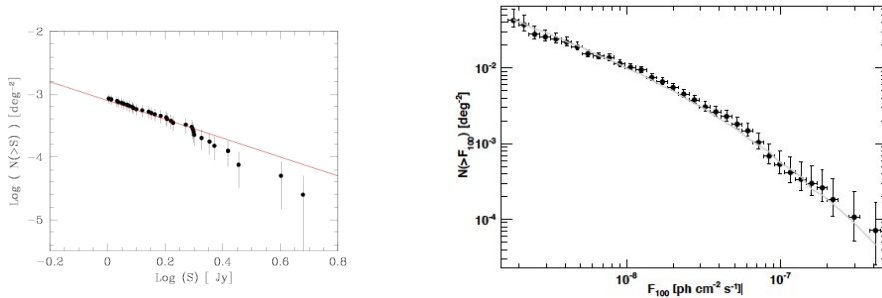


Fig. 3 Left: Integral number counts for the 1 Jy BLLs compared with the Euclidean relationship (red solid line). Adapted from Stickel et al. (1991). Right: Integral number density of BLLs from Fermi (from Ajello et al., 2014).

3.2 Luminosity Functions and parent population

The knowledge of the luminosity function of BLLs is instrumental to quantifying the beaming and thus to identifying the parent population. Its construction and evolution (redshift dependence) are more complicated than for other classes of AGN, because of the difficulty of distance determination, and of the consequences of the radiation beaming (Urry & Shafer, 1984; Maccacaro et al., 1984; Urry & Padovani, 1991; Caccianiga et al., 2002; Marchã & Caccianiga, 2013). The luminosity functions of BLLs at radio and X-ray frequencies had been evaluated, often with the purpose to compare them with those of radiogalaxies, in search of similarities that could prove the direct link between the two classes, under the assumption that they only differ in the viewing angle. A common result of these efforts is that BLLs and FSRQs can be plausibly connected to FR I and FR II radiogalaxies, respectively (Urry & Padovani, 1995; Rector et al., 2000; Chiaberge et al., 2001; Capetti et al., 2002), a conclusion that was independently reached also based on their similar host galaxies and environments (see also Sections 7 and 9), emission line intensities, and radio morphologies (for a review see Maraschi & Rovetti, 1994). The detailed comparison of radio and optical properties of BLLs and of their alleged parent population (radiogalaxies) might require more complex jet geometries (e.g. structured jets, Chiaberge et al., 2000; Trussoni et al., 2003).

The partial and sometime contradictory results obtained from the analysis of luminosity functions are plagued by the limited size of the original radio and X-ray samples (see e.g. Morris et al., 1991; Giommi et al., 1999; Rector et al., 2000; Caccianiga et al., 2002; Padovani et al., 2007; Marchã & Caccianiga, 2013). The current surveys in gamma-rays yield much more numerous samples. In their compilation of BLLs based on the first year of *Fermi* operations (Abdo et al., 2010a) Ajello et al. (2014) attempt to overcome the previous limitations by including BLLs with spectroscopic redshifts and BLLs with matching redshift estimates from broad-band photometry and intervening absorption systems spectroscopy (Fig. 3, right). Using this complete sample of 211 BLLs, they construct accurate gamma-ray luminosity functions of these sources. Their tentative outcome is that positive evolution is suggested for the majority of sources at luminosities larger than 10^{45} erg s⁻¹, while those at low luminosities may behave differently.

Their comparison with FSRQs (Ajello et al., 2012) suggests that the local ($z \simeq 0$) luminosity function of BLLs overlaps and connects smoothly to that of FSRQs, highlighting the similarity between the two classes, with BLLs having on average lower luminosity (and thus very likely lower Lorentz factors) than FSRQs. Ajello et al. (2014) also propose that BLLs correspond to the final (gas-starved, inefficiently accreting) and long-lasting phase of an earlier, short-lived, merger-driven, gas-rich epoch, represented by the FSRQs. A confirmation of this transition scenario can only rely on a more robust beaming correction and knowledge of the black hole masses and host galaxy environments, which are at present not well constrained.

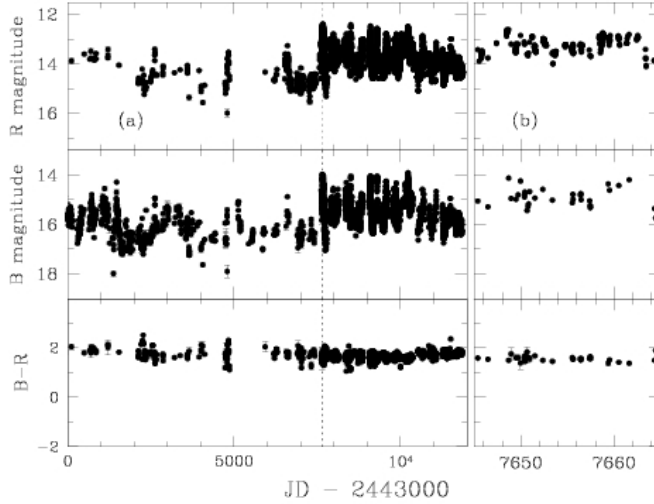


Fig. 4 (a) Light curves of BL Lacertae in R filter (top), B filter (middle) and $B - R$ color (bottom), during ~ 30 years since 1976. Flux variations of up to ~ 3 magnitudes are observed, while the color varies within ~ 1 magnitude. (b) Expanded view of variability during the 3-weeks period indicated as a vertical dashed line in panel (a). Variations of the order of ~ 1 magnitude are seen in a time-scale of few days, while the color remains almost constant. The light curves were produced using data from the WEBT archive (courtesy of C.M. Raiteri and M. Villata).

4 Flux variability

One of the distinctive properties of BLLs is high amplitude flux variability (up to 5 magnitudes) over a range of time-scales from months down to minutes (Miller et al., 1989; Wagner & Witzel, 1995). Variability is present over the whole near-infrared-to-ultraviolet range and does not exhibit periodic behavior; occasional outbursts of few magnitudes occurring in tens of days are observed. It is generally achromatic, in particular for sources with their synchrotron peak located at frequencies higher than the optical (Fig. 4).

While in the majority of AGNs the variability time-scale can be almost directly linked to the size of the central supermassive black hole and to the accretion rate (McHardy et al., 2006), in blazars this correlation does not hold because the luminosity is due to the highly anisotropic and relativistic

jet component, rather than to the accretion disk (see Section 1). The relativistic aberration magnifies the variation amplitudes and foreshortens the time-scales, so that small (10-20%) monthly or yearly flux changes, that are typical in radio-quiet quasars, become inter- or intra-day variations with amplitudes of a factor of up to 10 or more. Owing to the distance and to the extreme compactness of the regions at the base of the jet, where most of the radiation is emitted (the light-crossing times inferred from TeV observations are less than an hour), direct imaging of the nuclear zones, aimed at mapping the structure of the jet and the plasma outflow is not possible. Rapid variability and correlated variations of the emission at different wavelengths represent the only effective investigation tool of the jet geometry and dynamics. Ideally, these should be coupled with high angular resolution radio observations (VLBI) in order to correlate the flux variations at optical, X- and gamma-rays with the appearance and motion of new radio components moving across and away from the nucleus.

Multi-wavelength energy distributions and their variability provide some fundamental physical parameters, most of which are not model-dependent and can thus be considered solid, although affected by the measurement uncertainties and limitations. As an example, the cooling phase of an outburst (flux decrease) yields the average magnetic field, and the break frequencies of the synchrotron and inverse Compton spectral components give the electron energy. Their values constrain the jet models. Therefore, multi-wavelength observing campaigns of BLLs are organized in conjunction with outbursts, to study the jet behavior in these sources where its phenomenology is most pure and undiluted. Observations in the optical domain are crucial, because the emission at these wavelengths is “pristine”, i.e. not scattered or reprocessed, and rich, i.e. not “photon-starved” as it is often at X- or gamma-rays, where the photons are normally much fewer.

The first optical studies, started in the 1970’s, were based on measurements taken on photographic plates and with photomultipliers (Weistrop, 1973; Véron & Véron, 1976; Miller et al., 1978a; Miller & McGimsey, 1978; Westerlund et al., 1982; Sillanpaa et al., 1988a). More recently, CCD photometry has replaced the previous types of measurements almost entirely. Since BLLs are very bright (most of those at $z \lesssim 0.5$ have magnitudes in the range $V \sim 13 - 15$), accurate studies of variability are possible even with small telescopes (0.5-1m aperture) and indeed, the advent of robotic optical and infrared facilities, primarily oriented to the follow-up and monitoring of rapid transients (e.g. Gamma-Ray Bursts), has greatly benefitted the BLL field. These small telescopes (e.g., REM, ROTSE, SMARTS) have flexible schedules and pointing constraints, therefore they can be devoted to long looks of variable sources like BLLs (Tosti et al., 1996; Ciprini et al., 2003; Carini et al., 2004; Gu et al., 2006; Dolcini et al., 2007; Kastendieck et al., 2011; Ackermann et al., 2012; Bonning et al., 2012; Nesci et al., 2013; Sandrinelli et al., 2014).

In few cases, optical orbiting telescopes designed for long, uninterrupted monitorings, like Kepler, have been used for BLL variability studies (Edelson et al., 2013). Photometry from a satellite also presents the advantage of no

atmospheric contamination (“seeing”), which may be an issue at small variability amplitudes, where atmosphere instability may mimic intrinsic flickering. In the ultraviolet domain (1200-3000 Å), an important role for BLL monitoring was played in the past by the HST High Speed Photometer (Dolan & Clark, 2004) and especially by the IUE satellite, whose flexibility of scheduling and photometric stability made it apt for ultraviolet variability studies (Ulrich et al., 1984; Hanson & Coe, 1985; Maraschi et al., 1986; Edelson et al., 1991; Urry et al., 1993; Paltani & Courvoisier, 1994; Ghisellini et al., 1997; Heidt et al., 1997; Pian et al., 1997). Currently, *Swift*/UVOT, which couples good flexibility and sensitivity, is better suited for this class of studies than other ultraviolet orbiting facilities (Foschini et al., 2007; Perri et al., 2007; Pian et al., 2007; Tramacere et al., 2007; Raiteri et al., 2010; Aliu et al., 2013; H.E.S.S. Collaboration et al., 2012).

Often, optical and near-infrared monitorings of BLLs are organized as part of multi-wavelength campaigns, that have an emphasis on the X- and gamma-ray emission, and for which the information in the optical domain is crucial to reconstruct the broad-band spectrum for comparison with time-dependent modelling. This approach has reached a high degree of sophistication, thanks to the formation of consortia of optical observers (often including groups of amateur astronomers, Kato et al., 2004), who have made their expertise and resources available to this particular purpose. An instance of this is the *Fermi* - *AGILE* Support Program, organized within the Whole Earth Blazar Telescope⁷. While optical observations coordinated with wide multi-wavelength efforts cover generally outbursts and high activity states of BLLs (Raiteri et al., 2009), standalone optical programs may take place independently of the source flux state and thus offer an unbiased view of the source behavior in different states (Villata et al., 2002, 2004a).

As already mentioned, variations of BLL emission is seen on time-scales from minutes to many months and years, with amplitudes from a fraction of a magnitude to a factor of 100 or more (Tosti et al., 2002; Stalin et al., 2006; Zhang et al., 2008; Agudo et al., 2011; Gupta et al., 2012; Rani et al., 2013, e.g.). Modern observing techniques make it possible to correct reliably for spurious (non-astrophysical) causes of flux variations (e.g. atmospheric instabilities), even when these are small (micro-variability: < 0.1 mag, time-scales of less than one hour, Pollock et al., 2007). The vast majority of observed optical variations at all time-scales are intrinsic, i.e. not related to interstellar scintillation (irrelevant at optical wavelengths) or lensing by intervening sources, the role of which was proven to be inconclusive (Watson et al., 1999; Rector & Stocke, 2003; Giovannini et al., 2004; Raiteri et al., 2007).

Often, the rapid variability events violate the limits on efficiency of conversion of kinetic energy into luminosity (Guilbert et al., 1983), and/or are inconsistent, based on light-crossing times considerations, with independent estimates of the linear sizes of the inner emitting regions (e.g. Sandrinelli et al., 2014). This suggests lower limits on the Doppler boosting factors of the

⁷ GASP/WEBSITE, <http://www.oato.inaf.it/blazars/webt/>

order of $\delta \sim 10$, similar to those derived based on observed radio brightness temperatures and pair-production compactness at gamma-rays (see Section 1).

The correlated optical/near-infrared flux and spectral variability in BLLs can be complex, depending on the source state and on its broad-band spectrum (Abdo et al., 2010b; Nesci et al., 2013). Bonning et al. (2012) and Sandrinelli et al. (2014) report that the color-magnitude diagrams exhibit hysteresis cycles (as seen occasionally in X-rays, e.g. Takahashi et al., 1996; Fossati et al., 2000). The former authors also found somewhat larger amplitude variability at the optical than near-infrared wavelengths in BLLs, while the latter authors observed the opposite: this divergence is possibly related to the different time-scales probed. In low flux states, the optical/near-infrared energy distribution may deviate from a power-law shape and show an excess toward the short wavelengths (Sandrinelli et al., 2014), suggesting the presence of a thermal component, that is normally better detected in FSRQs.

The intra-day variations between different bands in BL Lacertae, the namesake of the class and a typical low-frequency-peaked object (according to the definition of Padovani & Giommi, 1995), are correlated without measurable time lags most of the time, and suggest that its optical variability properties remarkably resemble the X-ray variability properties of high-frequency-peaked BLLs. The similarities imply a common origin of the variations, plausibly the most energetic tails of the synchrotron emission produced by the relativistic electrons in the jets, for both the optical emission of low-frequency-peaked BLLs and the X-ray emission of high-frequency-peaked BLLs (Zhang et al., 2013b).

Time algorithms have been devised and applied to BLL light curves in search of characteristic time-scales, recurrences and to measure variability indices (Heidt & Wagner, 1998; Ciprini et al., 2003; Villata et al., 2004b; Bauer et al., 2009; Zhang et al., 2013a). These parameters give in turn insight into the behavior of the jet at different scales and they can be an effective tool to map its geometry, especially when coupled with information at other wavelengths. However, caution must be used in the interpretation of the outputs of correlation and auto-correlation functions and time structure functions in that often their features do not trace necessarily an authentic and intrinsic characteristic time-scale (Emmanoulopoulos et al., 2010). Unlike other fronts of research on BLLs that have progressed very quickly in the last two decades, the field of time analysis still presents facets that are not completely understood, so that despite the availability of advanced observing facilities that allow sophisticated monitorings in excellent conditions, the results are still inconclusive.

Periodicity has been searched for in the light curves of BLLs at all wavelengths on a wide range of frequencies and never been detected in a consistent way (Rieger, 2004; Osone, 2006). The only exception is OJ 287 ($z = 0.306$), for which a regular flux brightening recurrence every ~ 12 years was reported (Sillanpää et al., 1988b; Takalo, 1994) and confirmed by the detection of 9 equally spaced maxima - of which the latest 4 are very well sampled - in the optical light curve so far (see Fig. 5; Sillanpää et al., 1996; Hudec et al., 2013; Piha-joki et al., 2013a). The period is ascribed to the presence of a binary system

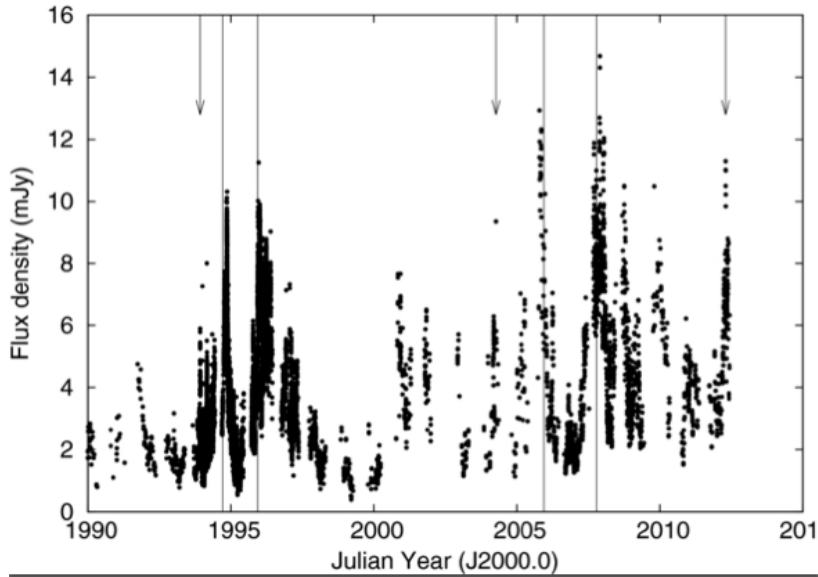


Fig. 5 Flux variability in the V band of OJ 287 over 25 years. Note the presence of a number of characteristic recurrent outbursts with an amplitude of an order of magnitude. The observed variability behavior was suggestive of some periodicity. The vertical lines represent the outburst timings from the model proposed by Pihajoki et al. (2013b).

of massive black holes at the center of the nucleus, that produce outbursts, often accompanied by precursors, when approaching pericenter (Valtonen et al. , 2008). In these occasions the flux may brighten by more than a factor of ~ 100 with respect to quiescence. Shorter-term variations with periodic and quasi-periodic character were also detected, that may be related to the matter dynamics in the close vicinity of the binary black hole system (Pihajoki et al., 2013b). On the other hand, Hudec et al. (2013) suggest maxima at times that are not foreseen by the model, making the interpretative picture not completely satisfactory.

5 Polarimetry

Blazars are the astrophysical sources with the highest percentage of optical linear polarization in the radio-to-ultraviolet range⁸. Unlike radio polarization, the optical polarized signal is immune from propagation effects like Faraday rotation of the polarization plane; moreover, optical polarimetry probes the central nuclear regions of blazar jets, where the radio emission is often self-absorbed.

⁸ The only other known sources showing similar polarization are optical counterparts of GRBs, at least during the first seconds to minutes after explosion, and indeed have in common with blazars the non-thermal origin of their continuum.

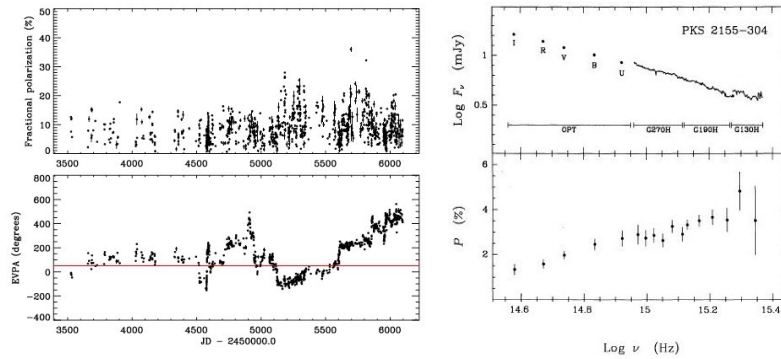


Fig. 6 Left: degree of polarization (top) and position angle (bottom) of the S5 0716+71 in October 2011 (adapted from Larionov et al., 2013). Right: HST and ground-based observations of the flux (top) and polarized degree (bottom) of PKS 2155-304 as a function of frequency. The fraction of polarization increases monotonically from optical to ultraviolet by a factor of ~ 2 . (adapted from Allen et al., 1993).

At optical and near-infrared wavelengths, the linear polarization percentage can be as high as 40% and it is normally detected at the level of 5-10% (Angel & Stockman, 1980; Takalo et al., 1992; Visvanathan & Wills, 1998; Tommasi et al., 2001a,b; Fujiwara et al., 2012; Pavlidou et al., 2013). Since blazar optical radiation is dominated by the synchrotron mechanism, this implies the presence of highly ordered large scale magnetic fields (Westfold, 1959). Circular polarization could be expected with a degree proportional to $1/\gamma$, where γ indicates the individual Lorentz factor of an emitting relativistic particle. Because of this it is very difficult to probe and detect (Takalo & Sillanpaa, 1993).

High linear polarization was very soon recognized as a distinctive feature of blazars, to the point that it has been adopted as a blazar selection criterion (Impey & Tapia, 1988; Impey et al., 1991; Smith et al., 2007; Hutsemékers et al., 2010; Heidt & Nilsson, 2011). Low-frequency-peaked BLLs and FSRQs are indistinguishable with regard to linear polarization and variability thereof (Visvanathan & Wills, 1998), while high-frequency-peaked BLLs are somewhat less polarized. This partially confirms the pioneering study of Angel & Stockman (1980).

Since interstellar dust can spuriously polarize the optical light, the detection of linear optical polarization percentage must be accurately corrected for this effect by estimating the amount of intervening dust. On the other hand, the host galaxy stellar light may dilute the intrinsic polarization and lower it artificially, an effect that should also be corrected for (Andruchow et al., 2008). However, variability of the polarized signal – which is often observed in BLLs – is a proof of its intrinsic origin.

Observations of optical polarization of BLLs have clearly shown that the degree of polarization varies on time-scales from intra-day to years (Fig. 6, left), with amplitudes from 20% to a factor of 2 (Impey & Tapia, 1988; Tom-

masi et al., 2001a,b; Hagen-Thorn et al., 2008). In some cases, even faster variations were claimed (Impey et al., 2000; Sasada et al., 2008). This variability is consistent with relativistically beamed synchrotron emission viewed at a very small angle to the line of sight.

Although the polarized optical light variations of BLLs are occasionally well correlated with those of the total light (Sorcia et al., 2013), in general lack of correlation or anti-correlation is observed (Gaur et al., 2014). Barres de Almeida et al. (2010) proposed that while the optical flux originates in the weakly polarized, stable jet component, the photopolarimetric variability results from the development and propagation of a shock in the jet. As a consequence, the optical polarized emission is potentially a better tracer of the high-energy emission, revealing the importance of optical polarimetric monitoring in multi-wavelength campaigns. Among these, some of the richest from the point of view of polarimetric coverage were presented by Urry et al. (1997), Tosti et al. (1998), Pietilä et al. (1999), Marscher et al. (2008), Agudo et al. (2011), Larionov et al. (2013), Itoh et al. (2013), Raiteri et al. (2013). These campaigns were often coordinated with VLBI monitoring of the radio components, and it was noted that the polarization variability events were often correlated with the crossing of the central core by a radio-emitting blob. In particular, the optical polarization angle settles on the direction parallel to newly born radio knot. The observed multi-wavelength behavior of the outbursts can be explained within the framework of a shock wave propagating along a helical path in the blazar’s jet (Camenzind & Krockenberger, 1992; Larionov et al., 2010; Zhang et al., 2014).

In few cases spectropolarimetry of bright BLLs was obtained in optical and ultraviolet and suggested a monotonic increase of polarization percentage towards shorter wavelengths (Fig. 6, right). From these measurements there is no evidence for the presence of an accretion disk or other thermal source contributing significantly to its ultraviolet continuum (Allen et al., 1993; Smith et al., 1993).

6 Spectroscopy

The (quasi) featureless optical spectra of BLLs are historically the main characteristic for this class of objects, that distinguishes them within the blazar family (see Section 1). This peculiarity made them rather elusive, because of the consequent difficulty to determine their redshift and thus the distance. However, it was early recognized that for a number of low redshift BLLs it was possible to detect faint absorption and/or emission features (see e.g., Miller et al., 1978a,b, and also Section 7) that allowed one to prove the extragalactic nature of the sources and assess their redshift. For low redshift targets the optical spectra (see example in Fig. 7) left no doubts that the BLL phenomenon occurs in the nuclei of galaxies dominated by old stellar populations (Ulrich, 1978), a result that was also confirmed by first imaging studies (see Section 7 for details). In most cases, however, the high luminosity of the non-thermal

emission from the nucleus with respect to the light from the underlying nebula yields spectra with very weak lines. When observed with poor signal-to-noise ratio and resolution their optical spectra appear therefore featureless (see example in Fig. 8).

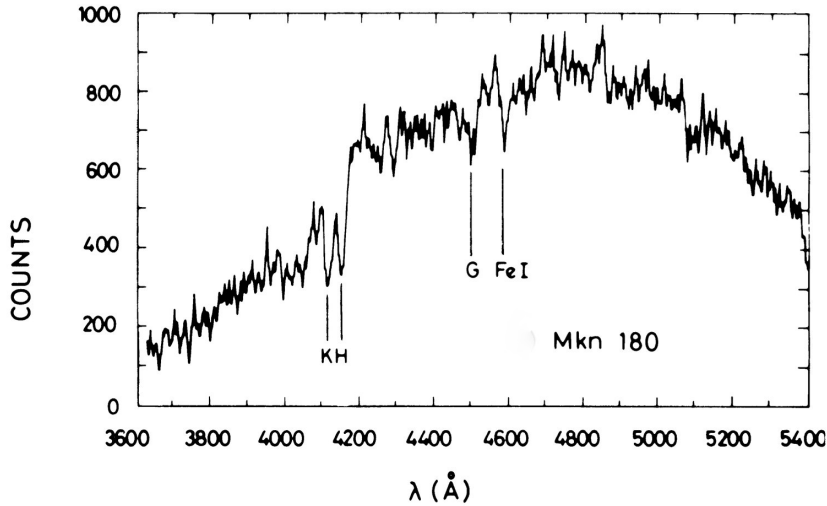


Fig. 7 The optical spectrum of the BL Lac object Markarian 180 obtained with the first generation of digital detectors. Absorption features from the host galaxy at $z = 0.046$ are clearly detected (Ulrich, 1978).

The spectral features of BLLs can be grouped into three types: 1) spectral lines of stars from the host galaxy; 2) weak emission lines characteristic of low density gas; 3) intervening absorptions from cold gas. While from the first two types a redshift can be derived, in the latter case only a lower limit on the redshift can be obtained. The faintness of intrinsic absorption or emission lines strongly depends on the brightness level of the nuclear source that is dominated by the jet component. Given the significant flux variability of the nuclear source (see Section 4), the detection of features in the spectra depends on the brightness state of the BLL. Faint states favour the detection of intrinsic emission lines while during high states intervening absorptions may be more easily detected because of the better signal-to-noise ratio.

6.1 Broad emission lines

Although the optical spectrum of BLLs is characterized by a featureless continuum, in a number of cases (see example in Fig. 9) weak broad emission lines, similar to those observed in quasars but at lower intrinsic luminosities, are seen. Owing to the weakness of these lines they may be detectable depending on the state of the source and the quality of the observations. Such

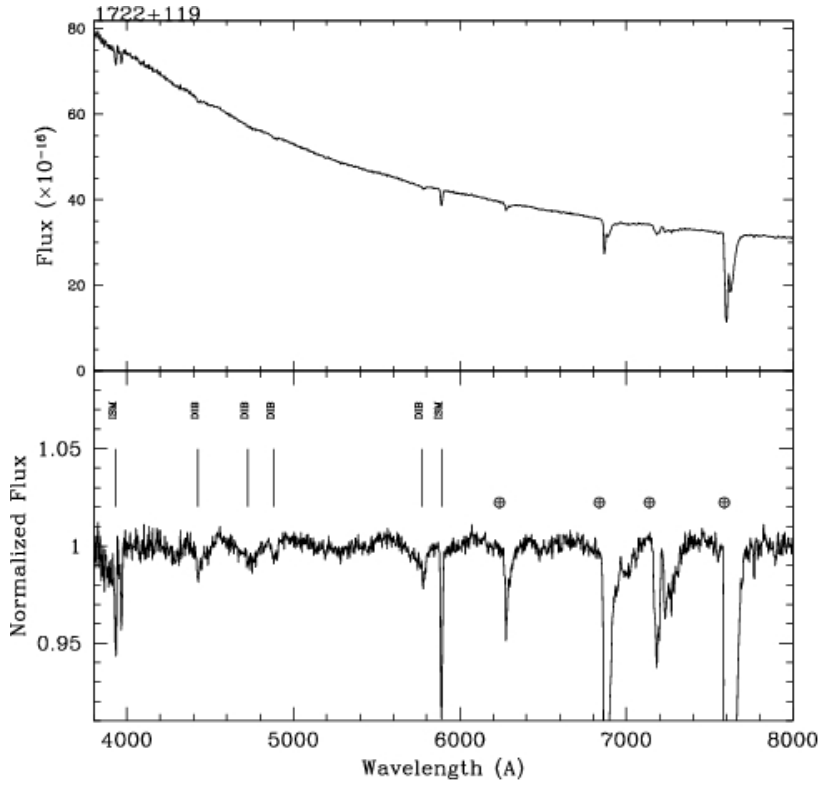


Fig. 8 The flux calibrated (top panel) and continuum-normalized (bottom panel) optical spectra of H 1722+11. The only absorption features besides the telluric bands are due to the Galactic interstellar medium: Ca II $\lambda\lambda$ 3934, 3968 and Na I λ 5892 atomic lines and DIBs at 4428, 4726, 4882, and 5772 Å (Sbarufatti et al., 2006b). See <http://archive.oapd.inaf.it/zbllac/> for more examples.

broad emission lines were occasionally found also in the prototype of the class, BL Lacertae (Vermeulen et al., 1995; Corbett et al., 1996).⁹ Comparing the spectra of BLLs and FSRQs it was found indeed that there is a continuity of emission line properties between the two sub-classes of blazars (Scarpa & Falomo, 1997), depending on the relative strength of the various involved components (jet emission, thermal disk or broad line region emission, host galaxy). It turns out therefore that the classification of an object as BLL or FSRQ may depend on the spectroscopic adopted criteria (see e.g. Padovani et al., 2012, for a detailed discussion on this issue). The emission line photons may be comptonized by both cold and relativistic electrons in the jet (external Compton, Sikora et al., 1994). While in FSRQs, owing to their conspicuous broad emission line luminosity, this is the dominant mechanism for production

⁹ As an aside, the detection of a broad H α emission line at the redshift of the host galaxy of BL Lacertae proved that the BLL prototype is not a high-redshift micro-lensed quasar (Ostriker & Vietri, 1985, 1990).

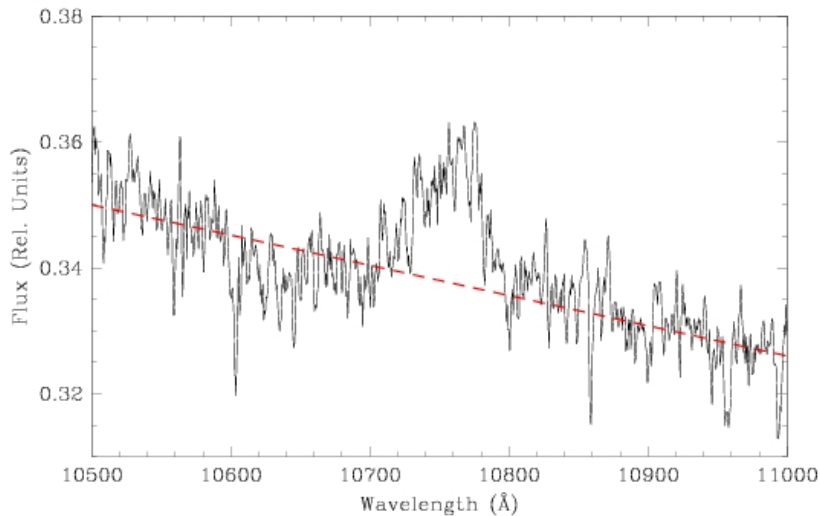


Fig. 9 The optical spectrum of PKS 0048-09 showing a very faint (equivalent width $\simeq 3 \text{ \AA}$) broad (2000 km s^{-1}) emission line of $\text{H}\alpha$ at $z = 0.638$. The power-law spectral continuum is shown as a red dashed curve (Landoni et al., 2012). See <http://archive.oapd.inaf.it/zbllac/> for more examples.

of gamma-rays, in BLLs it never exceeds significantly self-Comptonization of synchrotron radiation.

6.2 Host galaxy lines

As discussed in Section 7 virtually all BLLs reside in massive elliptical galaxies (or galaxies with a prominent spheroidal component). This means that their stellar population is dominated by old stars and the main absorption features are Ca II 3934,3967, G band 4304, H_β 4861, Mg I 5175, NaI 5875. These lines can be detected over the non-thermal component depending on the relative power of the two components (non-thermal and host galaxy) and on the signal-to-noise ratio and spectral resolution of the observations. Early spectroscopic studies of BLLs (see e.g., Ulrich, 1978) were limited by relatively modest spectroscopic capabilities and many objects remained therefore classified as featureless. Only for objects at low redshift and with faint nuclei these absorption lines could be observed since the bright continuum swamps the thermal component thus reducing significantly their equivalent width. High quality spectroscopic observations obtained with large telescopes (Sbarufatti et al., 2005, 2006a; Landoni et al., 2012; Sandrinelli et al., 2013; Shaw et al., 2013) improved significantly the ability to discover faint features from which the redshift is derived (see example in Fig. 10)

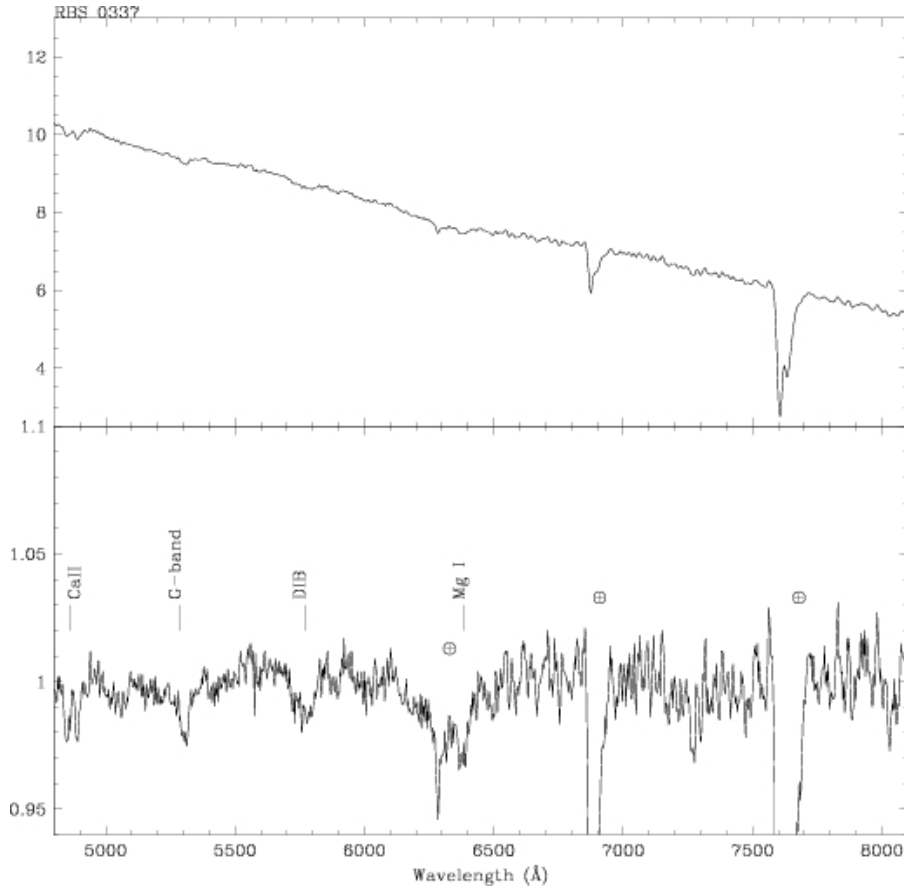


Fig. 10 The optical spectrum of RBS 0337 obtained at VLT (Landoni et al. (2012)). Superposed on the bright non-thermal emission are a number of faint absorption lines from the stellar population of the host galaxy. Telluric and interstellar medium features are also marked. The bottom panel shows the normalized spectrum. See <http://archive.oapd.inaf.it/zbl/ac/> for more examples.

In very few cases high quality spectroscopy secured with high spatial resolution probed ongoing star formation in the inner region of the host galaxy through the detection of narrow emission lines. A noticeable case is PKS 2005-489 ($z = 0.071$) for which spatially resolved emissions were observed in an extended rotating ring, perpendicular to the position of the radio jet, at 4 kpc from the nucleus. The presence of this rotating star-forming region is the signature of a minor accretion event that has funneled gas toward the central few kiloparsec region around the active nucleus (Bressan et al., 2006).

6.3 Intervening features

As in the case of high redshift quasars, gas along the line of sight to BLLs may produce absorption systems at a number redshifts lower than the redshift of the object. Since BLLs exhibit very weak or no intrinsic absorption lines, they are ideal sources for studying intervening absorptions. In particular they may be due to the Galactic interstellar medium. In the optical the Ca II and Na I are noticeable, together with diffuse interstellar bands (DIB) of molecular origin. An example is given in Figure 8.

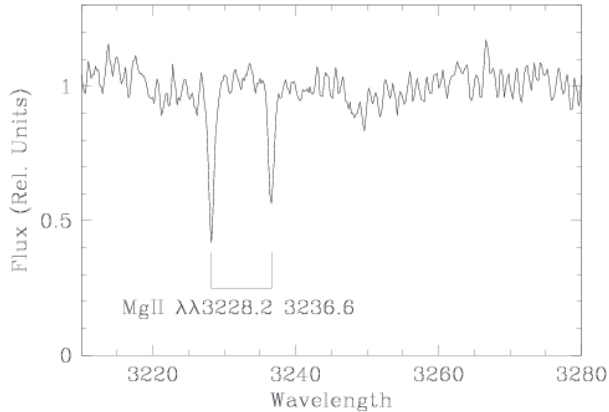


Fig. 11 ESO VLT X-Shooter optical spectrum of PKS 0048-09 ($z = 0.635$) showing intervening Mg II absorption doublet at $z = 0.154$ (Landoni et al., 2012)

The bulk of baryonic matter ($\sim 90\%$) probably resides around and between galaxies at low redshifts. A large fraction of it ($\sim 40\%$) is at high temperature ($T > 10^6 K$). It has been probed through the observation of O VII and O VIII and other X-ray absorption lines. In particular we recall here the observations of the bright BLL PKS 2155–304 (e.g. Nicastro et al., 2002; Cagnoni et al., 2004). At lower temperatures ($< 10^4 K$) the intervening gas can be traced by the Ly α forest absorption, while absorptions associated with galaxies halos are detected from metals (mainly Mg II and C IV). Relevant results in connection with BLLs and this line of research are consequent to the installation into HST of the Cosmic Origin Spectrograph (COS), which is a medium-high ($R \sim 10000$) resolution instrument of unprecedented sensitivity (e.g. Green et al., 2012).

So far, spectra of four BLLs (PG 1553+113, S5 0716+714, 3C 66A, and PG 1424+240) of previously unknown redshift were obtained in the wavelength range 1135–1795 Å. The data show a smooth continuum, with narrow ($\sim 100 \text{ km s}^{-1}$) absorption features arising mainly from the Lyman series. The redshift of each Ly α absorber can be measured in the $0 \lesssim z \lesssim 0.43$ interval. The maximum redshift yields immediately a lower limit to the redshift of

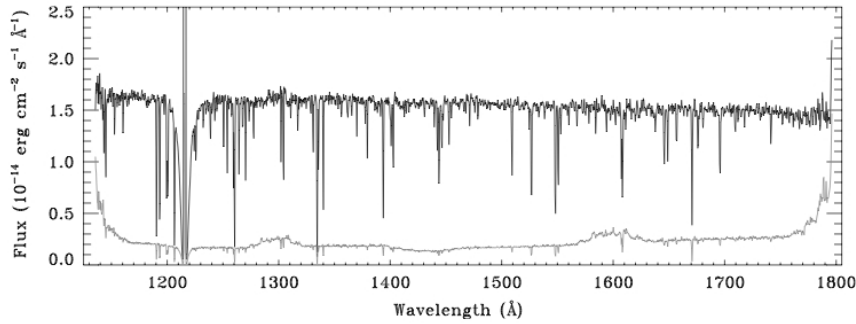


Fig. 12 Ultraviolet COS spectrum of PG 1553+113. Several narrow Lyman absorption line systems at different redshifts are observed (Danforth et al., 2010). A lower limit on the redshift of the BLL can be obtained from the distribution of the redshifts of the absorption systems.

the BLL, while an upper limit is derived from the expected distribution of the absorbers. An example of a spectrum is given in Figure 12. An important aspect of these findings is that all sources are GeV emitters (three of them are also TeV emitters). At TeV energies and $z \sim 0.4$, the opacity of the extragalactic background light for pair production is > 1 (see Section 2). Using this technique a TeV source (PG 1424+240) was found at $z > 0.6$. The redshifts derived from COS data, together with the gamma-ray spectra are therefore an effective powerful probe of the extragalactic infrared background (e.g. Costamante, 2013, and references therein).

A similar technique can be applied using Mg II $\lambda 2800$ absorption doublet, which at $z > 0.15$ can be observed from the ground. In Figure 11 we report the ESO VLT X-Shooter optical spectrum of PKS 0048-09 where a Mg II absorption at $z = 0.154$ is apparent.

7 Host galaxies

Soon after their discovery, it was noted that BLLs could be surrounded by a faint luminosity (Disney, 1974; Disney et al., 1974; Stein et al., 1976; Miller & Hawley, 1977). In the late 1970s the use of modern detectors (CCD) allowed observers to probe with better accuracy the nature of the nebosity (e.g. Fig. 13). Weistrop et al. (1979) imaged the BLL PKS 0548-322 in various filters and found it to be composed by a giant elliptical galaxy ($M_V \sim -22$) with a bright nucleus. About 10 years later, at the second conference entirely dedicated to BLLs in Como, M-H. Ulrich (Ulrich, 1989) reported about 15 objects for which a host galaxy was measured and compared their properties with those of bright radio galaxies in order to test the consistency of the hypothesis that BLLs are indeed the parent population of FR - I radio galaxies with the jet pointing closely to the observer direction. With the caveat of the exiguity and

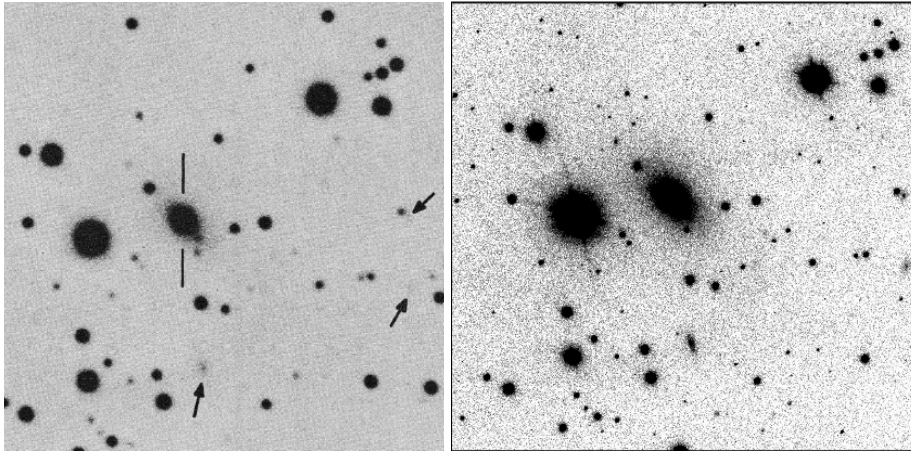


Fig. 13 Left: BL Lacertae as imaged in a photographic plate (Kodak IIA-J) in 1974 at the prime focus of Kitt Peak 4m telescope (Kinman, 1975). The target, indicated by two vertical lines, is clearly elongated and surrounded by a faint nebulosity. Arrows mark faint extended sources. Right: The same field as imaged in the R filter and CCD detector by the 2.5m Nordic Optical Telescope in 1998.

non-homogeneity of the dataset it was argued that the BLL host population is very similar to that of radiogalaxies.

The following decade has seen a significant improvement in terms of quality and sample size of BLL host galaxies. Various authors (Abraham et al., 1991; Stickel et al., 1993; Falomo, 1996; Wurtz et al., 1996; Falomo & Kotilainen, 1999) undertook ground based optical imaging studies of sizeable samples of objects including radio and X-ray-selected objects, according to the old definition. All these observations led to the conclusion that BLLs are the active nuclei of giant/massive elliptical galaxies with average luminosity in the R band $M_R \sim -23$. Only very few cases were reported to be different from this scheme suggesting that the host is a disk dominated galaxy (example: 1415+255; 1413+135; Stocke et al., 1992; Halpern et al., 1986) but these cases were rather controversial and mostly due to the modest angular resolution of the images (see e.g. Gladders et al., 1997; Falomo et al., 1997a; Lamer et al., 1999).

Optical observations were also complemented by near-infrared images, that would favour the detection of the host galaxy with respect to the nuclear emission owing to the difference of the ratio of the two components. This is more relevant for relatively high redshift sources since the emission from the host galaxy peaks in the near-infrared while in the optical band the light from the underlying stellar population diminishes significantly for objects with $z > 0.4-0.5$. Near-infrared observations of BLLs were collected by Wright et al. (1998) and Kotilainen et al. (1998) who extended the sample of resolved objects confirming previous results derived from optical studies. Moreover in a number of cases both optical and near-infrared images were available thus

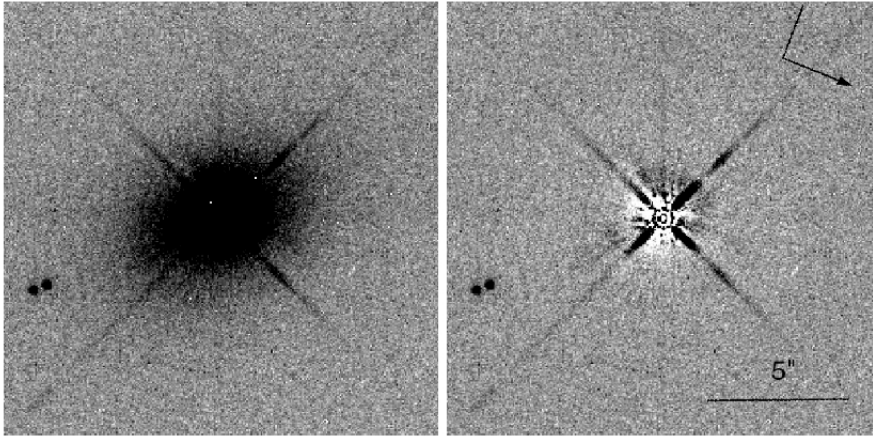


Fig. 14 Image of BL Lacertae obtained by HST (left) compared to galaxy-model subtracted image (right). No significant residuals are detected after the subtraction of the model (point source plus elliptical galaxy, convolved with the point spread function). The cross-shaped residuals are due to the diffraction pattern of the HST point spread function, which is not fully described by the two dimensional modelling (Falomo et al., 2000).

allowing the estimate of the integrated broad band color (R-H) on BLLs hosts. It turned out that the color is indistinguishable from that of inactive elliptical galaxies of similar luminosity (Kotilainen et al., 1998).

In spite of these imaging studies a significant fraction of observed objects remained unresolved and often these targets are also of unknown redshift. This is because, in order to disentangle the light of the host galaxy from that of the bright nucleus it is mandatory to observe the nuclei with the best possible angular resolution (i.e. narrow point spread function) and also have adequate signal-to-noise ratio in order to characterise the faint extended emission around the nucleus.

This achievement became possible with the observations of the refurbished HST and WFPC2. The first images of BLLs (Falomo et al., 1997b; Jannuzi et al., 1997; Urry et al., 1999) clearly demonstrated the great advantage of the HST angular resolution in characterizing the properties of the galaxies (see example in Fig. 14). The success of the first images prompted the acquisition of a large dataset of images through an HST snapshot program. Using the WFPC2 in the F702W filter short exposure (300-1000 s) images of 110 BLLs were secured (Scarpa et al., 2000). These form the largest and most homogeneous dataset of BLLs high resolution images. In this dataset it was possible to resolve all BLLs at redshift < 0.5 and many others at higher redshift or

with unknown z . All resolved host galaxies were found to be well fitted by an elliptical model (or with a dominant bulge component) and exhibited a relatively narrow range of absolute magnitude ($M_R = -23.0 \pm 0.6$; Urry et al. , 2000) with no significant difference depending on the original selection procedure (radio or X-ray). Comparison with the properties of nearby radiogalaxies strongly supports the unification picture with FR I galaxies as a favorite parent population (Urry & Padovani , 1

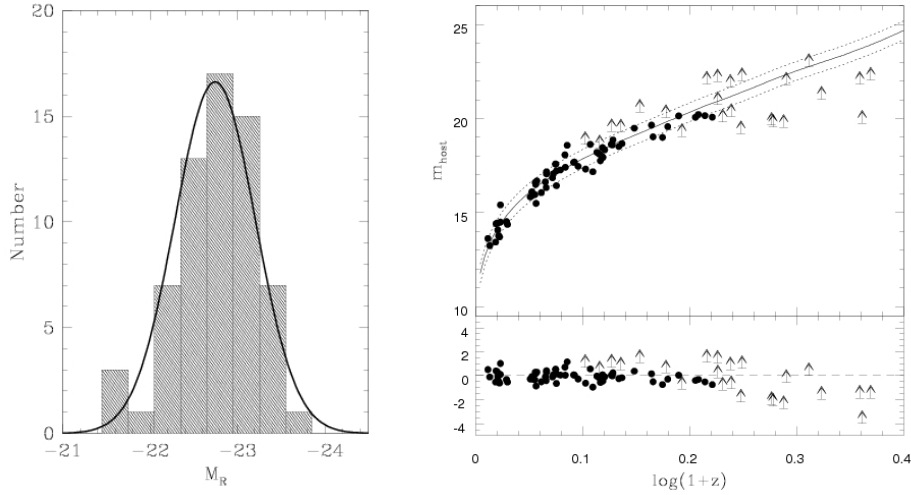


Fig. 15 Left: Distribution of the host galaxy absolute magnitudes M_R of BLLs from HST observations (Sbarufatti et al., 2005). The solid line represents a Gaussian fit to the distribution (mean $M_R = -22.9$). Right: Hubble diagram for host galaxies of BLLs (filled circles). Magnitude limits on unresolved host galaxies are indicated with arrows. The solid line corresponds to a galaxy of $M_R = -22.9$. Dotted curves show a 0.5 magnitudes spread. The scatter of the observed data with respect to the solid line is shown in the lower panel (see Sbarufatti et al., 2005, for details).

A detailed morphological analysis of the nearest ($z < 0.2$) objects (Falomo et al., 2000) revealed that the host galaxies are mostly smooth and unperturbed ellipticals with no signature of dusty features or sub-structures, albeit with a high incidence of close companions (see Fig. 14). It suggests that strong gravitational interaction is not relevant for the ongoing activity. Moreover in all cases the nucleus was found very well centered on the main body of the galaxy arguing against a microlensing hypothesis for the interpretation of the class (Ostriker & Vietri, 1985) .

The characterisation of the host galaxies could also help to constrain the distance of the objects in the cases of pure featureless optical spectra. To this aim it is mandatory to use high quality images of the targets. From the whole ensemble of imaging studies of BLLs, it turned out that the range of absolute magnitudes of the host galaxies of this class of AGN is relatively narrow and therefore one can use their luminosity as a sort of *standard candle*. Under this

assumption (see Fig. 15) if the host is detected then one can derive the *imaging redshift* from the apparent magnitude of the host galaxy. The method, initially proposed and applied to ground based images (Romanishin, 1987; Falomo, 1996; Falomo & Kotilainen, 1999) was then expanded and perfected using HST images (Sbarufatti et al., 2005). Providing that the photometric and structural properties of the host galaxies are well determined (by high quality images) the method is relatively robust and can yield redshift estimate with an average accuracy of $\Delta z \sim 0.05$ (see Figure 4 in Sbarufatti et al., 2005). Also in the case of non detection of the host galaxy it is possible to set constraints on the minimum redshift of the object (see e.g. Treves et al., 2007).

8 Jets

Radio-loud AGNs are often associated with jets. The quasar prototype 3C 273 was very early recognized to exhibit an optical jet structure (Schmidt, 1963). In the case of BLLs this association is even more cogent, since they are characterised by relativistic jets pointing in the observing direction (see Blandford & Rees, 1978, and Section 1). Nevertheless, the very fact of being pointed to the observer may make the study of the jet morphology rather elusive. In the radio band, thanks to the high angular resolution, jet detection is possible and in fact a large fraction of objects classified as BLLs show the signature of a jet, often with evidence of superluminal motion (see e.g. Giroletti et al., 2004). The arcsec structures are well studied with VLA or similar instruments (Ulvestad & Antonucci, 1986; Laurent-Muehleisen et al., 1993). Radio jet sub structures are commonly detected with milliarcsec resolution when observed with the VLBI (Ojha et al., 2010; Piner et al., 2010, and references therein). At $z \sim 0.1$ one can thus explore structures down to parsec scale.

Some counterparts are found also in X-rays in Chandra images (angular resolution ~ 1 arcsec) at relatively high redshift. They are interpreted as a result of the Compton scattering cosmic microwave background photons off the most energetic electrons (Schwartz et al., 2000; Tavecchio et al., 2000; Celotti et al., 2001). Jet morphology in X-ray was studied in some details for a number of close-by BLLs, like PKS 0521–365 (Birkinshaw et al., 2002), and PKS 2201+044 and 3C 371 (Sambruna et al., 2007), which notably are systems where the beaming is supposed to be modest. Knot structures are observed.

On the other hand, the jet is rarely detected in the optical and near-infrared bands. This depends both on the more limited angular resolution with respect to the radio band and on the short lifetime of the high energy electrons producing the non-thermal emission of the jet. Because of the requirements on spatial resolution, in the optical and infrared the jet morphology was mainly studied with HST (Scarpa et al., 1999) and more recently with adaptive optics methods (Falomo et al., 2009). A detailed study of the optical jet based on HST images was completed for PKS 0521–365, PKS 2201+04 and 3C 371 (Scarpa et al., 1999). In Figure 16 we show an example of optical jet of the

BLL PKS 0521–365 ($z = 0.0554$) superposed onto the prominent massive host galaxy.



Fig. 16 Combined color image (optical by HST + WFPC2; near-infrared by VLT + MAD) of the jet of PKS 0521–365. The jet is clearly structured with the closest knot at $\sim 1.5''$ from the bright nucleus. The inner part of the giant elliptical galaxy that hosts this BLL is also apparent. The faint red tip emission on the top right is not associated with the jet (see Falomo et al., 2009, for details).

Detailed analysis of the jet structure at radio, near-infrared and optical frequencies reveals a number of knots (see Fig. 17) that exhibit remarkable similarity at all frequencies (Falomo et al., 2009).

9 Environments

After the recognition that BLLs are hosted in elliptical galaxies an obvious further step was to search for associated groups or clusters of galaxies. Early suggestions of such association in the case of PKS 0548–322 (Disney, 1974) turned out to be false (but see below for surprise) and few other cases were suggested for 3C66A, AP Lib, PKS 1400+164 (Butcher et al., 1976; Visvanathan & Griessmith, 1977; Weistrop et al., 1983) but not properly confirmed. For instance in the case of 1440+164, for which an association with a group of galaxies was claimed, deep images obtained with modern instrumentation complemented by spectroscopy of a number of these galaxies showed that the group is not physically associated with the BLL (Pesce et al., 1994).



Fig. 17 The contour plot of the jet of PKS 0521–365 observed by HST+WFPC2 in R band (left), VLT + MAD in the K_s band (middle) and VLA at 15 GHz (right). The large star represents the position of the (subtracted) nucleus in both optical and near-infrared band (Falomo et al., 2009).

It was 25 years after the discovery of the BLL class that a number of systematic studies of the cluster environments around BLLs were undertaken. Using optical images Fried et al. (1993) performed a study of the galaxy density for the 1 Jy sample and found an increased galaxy density for low ($z \sim 0.3$) and intermediate ($z \sim 0.6$) redshift sources but not for higher redshift objects ($z \sim 1$). However, for the latter subsample their images were not deep enough to probe adequately the environments. Subsequent studies (Wurtz et al., 1993; Smith et al., 1995; Wurtz et al., 1997) showed that on average BLLs inhabit poor galaxy environments (Abell richness class ~ 0). Attempts to compare

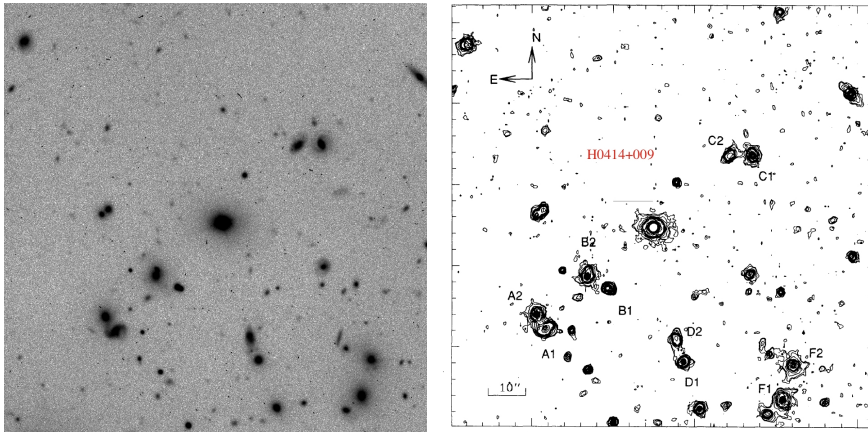


Fig. 18 Left: ESO NTT R-band image of the galaxies in the field of H 0414+009. Right: Contour plot of the image, showing galaxies at the same redshift as the BLL, forming a physical group of which the BLL host is the dominant member (Falomo et al., 1993c).

the environment properties with those of the alleged parent population (see Section 1) of FR I radiogalaxies yielded somewhat controversial results (Smith et al., 1995; Wurtz et al., 1997). All these studies were based only on photometry of the fields around the BLL sources, therefore the association with group of galaxies can be assessed only basing on statistical considerations. For a number of selected targets these imaging studies were complemented by spectroscopy of galaxies in the fields that demonstrated the physical association (same redshift) between the galaxies and the BLL source (see e.g. Falomo et al., 1993b,c; Pesce et al., 1994, 1995).

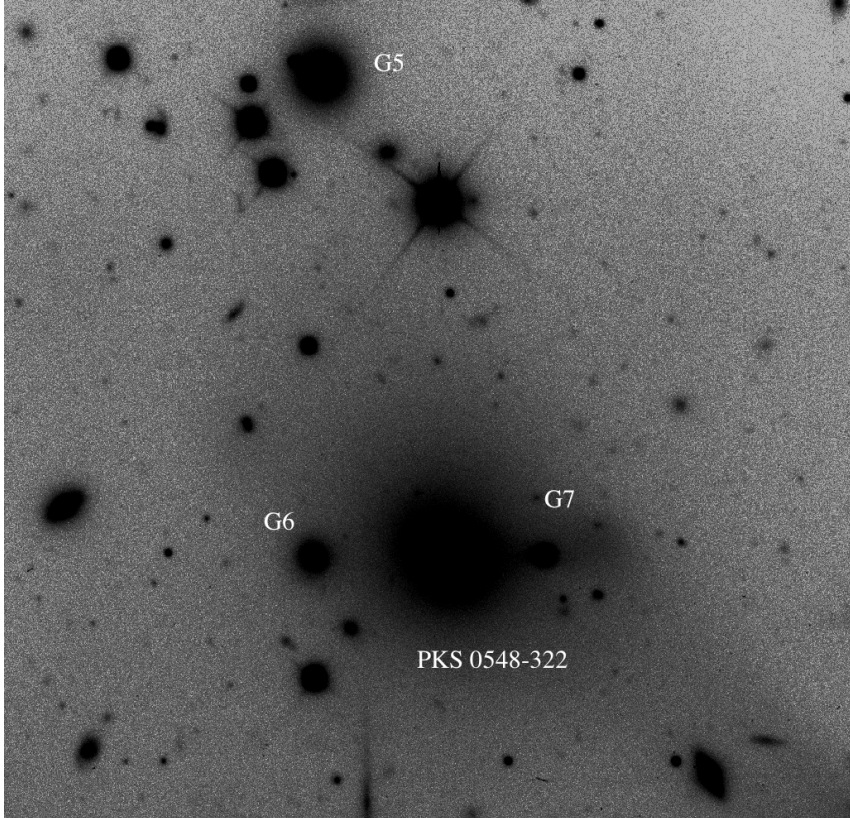


Fig. 19 The field around PKS 0548-441 imaged at ESO NTT + SUSI (R filter) showing the host galaxy and a number of galaxies at the same redshift as the BLL. This is a rare example of BLL associated with a relatively rich cluster of galaxies. (Falomo et al., 1995).

A interesting case of rich environment is found for the radio source PKS 0548-441. This target was among the first BLLs to be pointed out as likely connected with a cluster of galaxies at $z \sim 0.04$ (Disney, 1974). The claim was, however, soon disproved as the redshift of the source ($z = 0.069$) was derived (Fosbury & Disney, 1976). This nearby object was deeply investigated by

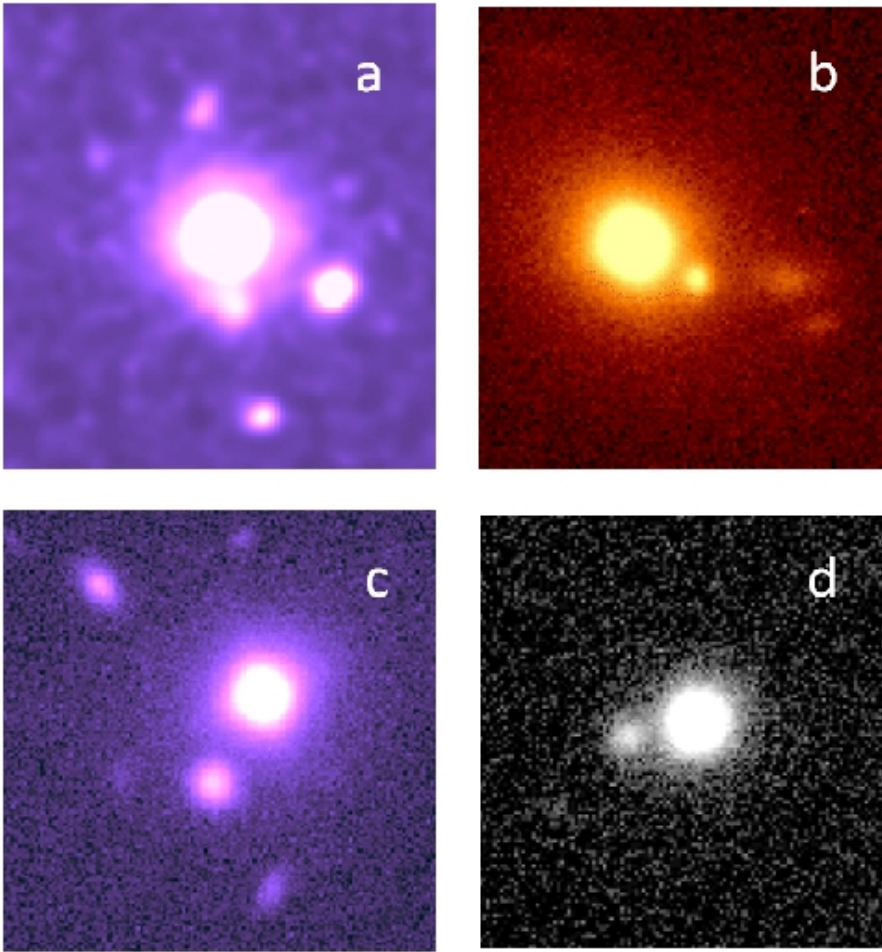


Fig. 20 Close (few arcsec angular distance) companions of BLLs (central bright objects): (a) PKS 0301-243: deconvolved image showing companions and a jet-like feature; (b) H 0323+022: distorted morphology and close companions; (c) PKS 0829+04: extended companions; (d) PKS 2335+031: close resolved companion galaxy (Falomo , 1996).

Falomo et al. (1995) who obtained both high quality images and spectroscopy of galaxies in the field . It turned out that the source is indeed located in a rich cluster of galaxies (see Fig. 19) of which the BLL host galaxy is clearly the dominant member with an absolute magnitude $M_R = -23.5$. The physical association of the cluster was proved by spectroscopy of many galaxies in the field that have the same redshift as the BLL source. This is a rare case of BLL object associated with a relatively rich (Abell class ~ 2) cluster of galaxies while most of the BLLs reside in poorer environments.

In spite of the relative bareness of BLL galaxy environment, it is rather frequent to find close companions within 10 arcsec (projected distance $< 20\text{-}50$ kpc for redshift in the range 0.1–0.4) from the target. Relevant examples are shown in Figure 20 (Falomo , 1996). In some cases the companion was found to be physically associated with the active nucleus (Falomo et al., 1993b, 1995; Heidt et al., 1999). However, owing to the faintness of the companions and their proximity to the bright BLL source, spectroscopy of the companions is lacking in many cases. Moreover in some cases also the redshift of the BLL target is unknown, and it is not possible to prove the association.

10 The black hole mass

In AGNs the mass of the black hole (M_{BH}) is a basic parameter characterizing the source. The standard paradigm is that AGN are supermassive accreting black holes (Salpeter , 1964; Zel'dovich , 1964). The mass fixes an upper limit to the AGN luminosity through the argument that the Eddington luminosity cannot be significantly overcome. If the accretion occurs through a disk, its inner radius depends on the mass, because it is related to the gravitational radius, and in turn this constrains the internal temperature. The disk inner dimension gives a number of natural time-scales, as the light crossing time, or the Keplerian time. The mass therefore enters as a basic parameter in the interpretation of the AGN variability.

The most widely used method to estimate the mass of quasars or Seyfert galaxies nuclei is based on the assumption that broad emission lines are produced by fluorescence of cold clouds irradiated by a central source, and orbiting the central black hole. The line width is related to the velocity of the clouds while the distance of the cloud may be derived from *reverberation mapping*, that yields the time delay between a flare in the continuum, and the response of a line flux which is produced in the cloud (Peterson , 1997). Because of the expensiveness of this method, alternatively one can use an experimental relationship (with significant dispersion) between the size of the broad line region and the luminosity of the continuum close to the emission line. This technique allowed the estimate of the mass of thousands of quasars with a precision of a factor ~ 3 (Shen et al. , 2011).

In the case of BLLs this method can be applied only to few sources showing broad emission lines and with particular caution, since the observed emission is dominated by a relativistic jet. Therefore it is of obvious importance to adopt other methods to estimate the black hole mass of BLLs. In the local Universe it was demonstrated that most galaxies contain in their center a massive black hole and that its mass is correlated with some properties of its host galaxy (luminosity, mass, velocity dispersion). As a rule of thumb the mass of the black hole is $\sim 0.1\%$ of that of the spheroidal component. The host galaxies of BLLs are supposedly giant ellipticals, i.e the whole galaxy coincides with spheroidal component. The mass of the ellipticals scales as the luminosity. Therefore one can construct a black hole vs host galaxy absolute magnitude

relationship, which can be used for establishing the mass once the host galaxy luminosity is measured.

In the case of BLLs the main difficulty is to measure the luminosity of the host galaxy (see Section 7). From systematic measurements of the host galaxies luminosity of BLL up to $z \sim 0.5$ the black hole masses have been calculated by Woo & Urry (2002) and Falomo et al. (2003b, see Fig. 21). Beyond that redshift limit the host galaxies become very difficult to detect, and evolutionary effects may become important, requiring corrections to the relations obtained locally.

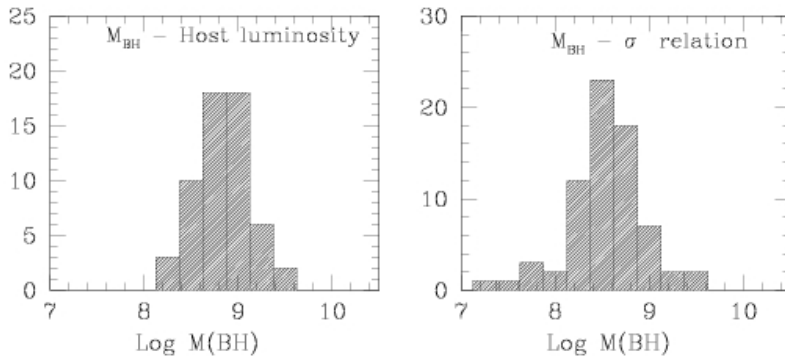


Fig. 21 Left panel: distribution of black hole masses of BLLs derived from the luminosity of their host galaxies (Falomo et al. , 2003b). Right panel: distribution of black hole masses from the $\sigma - M_{BH}$ relation (Plotkin et al. , 2011).

Another parameter of the host galaxy, which is related to the mass of the black hole is the velocity dispersion σ of the central part of the galaxy. It is measured through the width of the absorption lines (typically H_β) of the stellar component. In terms of dispersion the $\sigma - M_{BH}$ relation is somewhat preferable than that discussed in the previous paragraph. The technique for mass determination of BLLs was introduced by Falomo et al. (2002), in this way it was determined the mass of a dozen objects Falomo et al. (2003a) and Barth et al. (2003). It was extended to ~ 60 objects by Plotkin et al. (2011), who considered the sample of optically selected BLL candidates from the SDSS DR7 (see Section 3 and Fig. 21). Also in this case there is a maximum value of $z \sim 0.5$, for the applicability of the method, related to the possibility of having reliable measurements of σ . The mass distributions reported in Fig. 21 are very similar to those of quasars, as deduced from the width of broad lines and the continuum intensity (see e.g. Shen et al. , 2011).

Finally another technique, mutated from X-ray binaries, is based on Shakura-Sunyaev disk model (Shakura & Sunyaev , 1973). The idea is to consider the

spectral energy distribution of the source in a broad frequency range, exclude the contribution of the jet, and isolate the one from the accretion disk. In practice one should be able to observe the region where νF_ν has a maximum. The fit with a Shakura-Sunyaev disk allows one to constrain the mass and the accretion rate. If the redshift is known the latter quantity can be fixed and one obtains the mass. Up to now, results have been obtained for high redshift blazars ($z > 2$), rather than BLLs (Sbarrato et al. , 2013).

11 Concluding Remarks

About half a century after the discovery of the first BLLs the basic picture to interpret this enigmatic class of sources appears robust: BLLs are active nuclei of massive elliptical galaxies the emission of which is dominated by relativistic jets. The bright compact radio cores, high luminosities and rapid, large amplitude flux variability at all frequencies and the strong polarization that characterise these objects are well explained in this scenario. Also the observed quasi featureless optical spectra of BLL, that is one of the distinctive properties of the class, find a natural explanation in the above beaming model. At variance with other classes of AGN, like quasars and Seyfert galaxies, the lack of prominent spectral features was, and still in part is, a significant limiting factor for the determination of their redshift and ensuing evaluation of their physical properties. The implication of this model is the existence of a large number of misaligned objects with the same intrinsic properties as BLLs. The most obvious candidates are low-power radiogalaxies.

BLLs were mainly discovered as counterparts of radio and/or X-ray sources. The surveys in these bands led to the compilation of the first, albeit relatively small, complete samples of objects from which it was possible to start the exploration of the cosmic evolution of the class as compared with other types of AGN. Because of the limited number of known BLL and the paucity of known objects at high redshift ($z \gtrsim 1$) the evolution with cosmic time remains vague. Negative or positive evolution were suggested for different samples, although almost consistent with no evolution, yielding a picture substantially different from that of the majority of AGNs, where significant positive evolution is seen.

The investigation of the cosmic evolution of BLLs is an important issue that could offer relevant clues on the relationship between the formation of supermassive black holes and the development of relativistic jets. In order to achieve a significant progress in the understanding of the cosmic evolution of BLLs the extension of available samples to higher redshift is mandatory.

The discovery and follow-up study of high-redshift BLLs will come within reach thanks to the new generation of observing facilities at all frequencies foreseen for the next decades (e.g., Square Kilometer Array, Extremely Large Telescopes, James Webb Space Telescope, Large Synoptic Survey Telescope, Advanced Telescope for High Energy Astrophysics, Cherenkov Telescope Array). In particular, high signal-to-noise ratio spectroscopy of BLL candidates obtained with adaptive optics instrumentation at extremely large telescopes

in the near-infrared will allow one to observe the rest-frame optical spectrum of high-redshift sources and determine the redshift from absorption features of the host galaxies or faint emission lines. This will produce the first sizable high-redshift sample of BLLs, that, compared with the lower redshift samples, will yield a firm conclusion on cosmic evolution of the class. This could be related to the role of the angular momentum of the central black hole in forming a relativistic jet.

Although the observational knowledge of the BLL phenomenon is relatively well established, on the theoretical front some fundamental aspects remain unsolved. Specifically, a central problem of BLL physics is the mechanism for the extraction and transfer of energy from the inner engine to the jets. We trust that the observations with the above-mentioned future facilities will provide huge gain in terms of signal-to-noise ratio, spatial and time resolution for spectroscopy, photometry and polarimetry. Some examples of the expected capabilities for the determination of the redshift with future optical and near infrared facilities are given in Landoni et al. (2013) and Landoni et al. (2014).

These crucial measurements will also contribute to the comprehension of the mechanisms of conversion of rotational energy into kinetic energy of the jet and into luminosity in various channels (electromagnetic, neutrinos, gravitational radiation).

Acknowledgements We are grateful to Catherine Boisson, Alessandro Caccianiga, Stefano Covino, Luigi Foschini, Gabriele Ghisellini, Oliver King, Alan Marscher, Claudia Raiteri, Kenji Toma, Massimo Villata, Andreas Zech for inputs in the preparation of this work. In particular, we thank Gabriele Giovannini and Massimo Persic for useful suggestions, comments and discussions on this review. We are also very grateful to Angela Sandrinelli and Marco Landoni for a careful reading of the manuscript and for fruitful comments. We acknowledge support from ASI/INAF grant I/088/06/0 and PRIN MIUR 2010/2011.

References

- Abazajian, K. N., Adelman-McCarthy, J. K., Agüeros, M. A., et al. 2009, *Ap.J. Suppl.*, 182, 543
- Abdo, A. A., Ackermann, M., Ajello, M., et al. 2010a, *Ap.J.* , 715, 429
- Abdo, A. A., Ackermann, M., Agudo, I., et al. 2010b, *Ap.J.* , 716, 30
- Abraham, R. G., Crawford, C. S., & McHardy, I. M. 1991, *MNRAS* , 252, 482
- Acciari, V. A., Aliu, E., Arlen, T., et al. 2011, *Ap.J.* , 738, 169
- Ackermann, M., Ajello, M., Allafort, A., et al. 2011, *Ap.J.* , 743, 171
- Ackermann, M., Ajello, M., Ballet, J., et al. 2012, *Ap.J.* , 751, 159
- Agudo, I., Marscher, A. P., Jorstad, S. G., et al. 2011, *Ap.J. Letters*, 735, L10
- Aharonian, F. A. 2000, *New Astronomy*, 5, 377
- Aharonian, F., Akhperjanian, A. G., Anton, G., et al. 2009, *A&A* , 502, 749
- Ajello, M., Shaw, M. S., Romani, R. W., et al. 2012, *Ap.J.* , 751, 108
- Ajello, M., Romani, R. W., Gasparrini, D., et al. 2014, *Ap.J.* , 780, 73
- Aleksić, J., Antonelli, L. A., Antoranz, P., et al. 2011, *A&A* , 530, A4
- Aleksić, J., Alvarez, E. A., Antonelli, L. A., et al. 2012, *A&A* , 542, A100

- Aliu, E., Aune, T., Beilicke, M., et al. 2011, *Ap.J.* , 742, 127
- Aliu, E., Archambault, S., Arlen, T., et al. 2013, *Ap.J.* , 775, 3
- Allen, R. G., Smith, P. S., Angel, J. R. P., et al. 1993, *Ap.J.* , 403, 610
- Andruchow, I., Cellone, S. A., & Romero, G. E. 2008, *MNRAS* , 388, 1766
- Angel, J.R.P., & Stockman, H.S. 1980, *Ann.Rev.A.A.*, 18, 321
- Asano, K., Takahara, F., Kusunose, M., Toma, K., & Kakuwa, J. 2014, *Ap.J.* , 780, 64
- Barres de Almeida, U., Ward, M. J., Dominici, T. P., et al. 2010, *MNRAS* , 408, 1778
- Barth, A. J., Ho, L. C., & Sargent, W. L. W. 2003, *ApJ*, 583, 134
- Bauer, A., Baltay, C., Coppi, P., et al. 2009, *Ap.J.* , 699, 1732
- Beckmann, V., Engels, D., Bade, N., & Wucknitz, O. 2003, *A&A* , 401, 927
- Begelman, M. C., Blandford, R. D., & Rees, M. J. 1984, *Reviews of Modern Physics*, 56, 255
- Begelman, M. C., Fabian, A. C., & Rees, M. J. 2008, *MNRAS* , 384, L19
- Bersanelli, M., Bouchet, P., Falomo, R., & Tanzi, E. G. 1992, *A.J.*, 104, 28
- Birkinshaw, M., Worrall, D. M., & Hardcastle, M. J. 2002, *MNRAS* , 335, 142
- Björnsson, C.-I. 1990, *MNRAS* , 242, 158
- Blandford, R. D., & Znajek, R. L. 1977, *MNRAS* , 179, 433
- Blandford, R. D. & Rees, M. J. 1978, In: *Pittsburgh Conference on BL Lac Objects*, Pittsburgh, Pa., April 24-26, 1978, *Proceedings. (A79-30026 11-90)* Pittsburgh, Pa., University of Pittsburgh, 1978, p. 328-341
- Błażejowski, M., Sikora, M., Moderski, R., & Madejski, G. M. 2000, *Ap.J.* , 545, 107
- Böttcher, M., Reimer, A., Sweeney, K., & Prakash, A. 2013, *Ap.J.* , 768, 54
- Bonning, E., Urry, C. M., Bailyn, C., et al. 2012, *Ap.J.* , 756, 13
- Bressan, A., Falomo, R., Valdés, J. R., & Rampazzo, R. 2006, *Ap.J. Letters*, 645, L101
- Butcher, H. R., Oemler, A., Jr., Tapia, S., & Tarenghi, M. 1976, *Ap.J. Letters*, 209, L11
- Caccianiga, A., Maccacaro, T., Wolter, A., Della Ceca, R., & Gioia, I. M. 2002, *Ap.J.* , 566, 181
- Caccianiga, A., Severgnini, P., Della Ceca, R., et al. 2008, *A&A* , 477, 735
- Cagnoni, I., Nicastro, F., Maraschi, L., Treves, A., & Tavecchio, F. 2004, *Ap.J.* , 603, 449
- Camenzind, M., & Krockenberger, M. 1992, *A&A* , 255, 59
- Capetti, A., Celotti, A., Chiaberge, M., et al. 2002, *A&A* , 383, 104
- Carini, M. T., Barnaby, D., Mattox, J. R., et al. 2004, *Astronomische Nachrichten*, 325, 646
- Celotti, A., Ghisellini, G., & Chiaberge, M. 2001, *MNRAS* , 321, L1
- Chen, P. S., Fu, H. W., & Gao, Y. F. 2005, *Nature*, 11, 27
- Chen, P. S., & Shan, H. G. 2011, *Ap.J.* , 732, 22
- Chiaberge, M., Celotti, A., Capetti, A., & Ghisellini, G. 2000, *A&A* , 358, 104
- Chiaberge, M., Capetti, A., & Celotti, A. 2001, *MNRAS* , 324, L33
- Ciprini, S., Tosti, G., Raiteri, C. M., et al. 2003, *A&A* , 400, 487
- Corbett, E. A., Robinson, A., Axon, D. J., et al. 1996, *MNRAS* , 281, 737

- Costamante, L., Ghisellini, G., Giommi, P., et al. 2001, *A&A* , 371, 512
- Costamante, L. 2013, *International Journal of Modern Physics D*, 22, 30025
- Cusumano, G., La Parola, V., Segreto, A., et al. 2010, *A&A* , 524, A64
- D'Abrusco, R., Massaro, F., Paggi, A., et al. 2013, *Ap.J. Suppl.*, 206, 12
- Danforth, C. W., Keeney, B. A., Stocke, J. T., Shull, J. M., & Yao, Y. 2010, *Ap.J.* , 720, 976
- Disney, M. J. 1974, *Ap.J. Letters*, 193, L103
- Disney, M. J., Peterson, B. A., & Rodgers, A. W. 1974, *Ap.J. Letters*, 194, L79
- Dolan, J. F., & Clark, L. L. 2004, *Ap.J.* , 607, 84
- Dolcini, A., Farfanelli, F., Ciprini, S., et al. 2007, *A&A* , 469, 503
- Edelson, R. A., Saken, J., Pike, G., et al. 1991, *Ap.J. Letters*, 372, L9
- Edelson, R., Mushotzky, R., Vaughan, S., et al. 2013, *Ap.J.* , 766, 16
- Elvis, M., Plummer, D., Schachter, J., & Fabbiano, G. 1992, *Ap.J. Suppl.*, 80, 257
- Emmanoulopoulos, D., McHardy, I. M., & Uttley, P. 2010, *MNRAS* , 404, 931
- Falomo, R., Treves, A., Chiappetti, L., et al. 1993, *Ap.J.* , 402, 532
- Falomo, R., Pesce, J. E., & Treves, A. 1993, *Ap.J. Letters*, 411, L63
- Falomo, R., Pesce, J. E., & Treves, A. 1993, *A.J.*, 105, 2031
- Falomo, R., Bersanelli, M., Bouchet, P., & Tanzi, E. G. 1993, *A.J.*, 106, 11
- Falomo, R., Pesce, J. E., & Treves, A. 1995, *Ap.J. Letters*, 438, L9
- Falomo, R. 1996, *MNRAS* , 283, 241
- Falomo, R., Kotilainen, J., Pursimo, T., et al. 1997, *A&A* , 321, 374
- Falomo, R., Urry, C. M., Pesce, J. E., et al. 1997, *Ap.J.* , 476, 113
- Falomo, R., & Kotilainen, J. K. 1999, *A&A* , 352, 85
- Falomo, R., Scarpa, R., Treves, A., & Urry, C. M. 2000, *Ap.J.* , 542, 731
- Falomo, R., Kotilainen, J. K., & Treves, A. 2002, *Ap.J. Letters*, 569, L35
- Falomo, R., Kotilainen, J. K., Carangelo, N., & Treves, A. 2003, *Ap.J.* , 595, 624
- Falomo, R., Carangelo, N., & Treves, A. 2003, *MNRAS* , 343, 505
- Falomo, R., Pian, E., Treves, A., et al. 2009, *A&A* , 501, 907
- Fanaroff, B. L., & Riley, J. M. 1974, *MNRAS* , 167, 31P
- Finke, J. D., Dermer, C. D., Boettcher, M. 2008, *Ap.J.* , 686, 181
- Fleming, T. A., Green, R. F., Jannuzi, B. T., et al. 1993, *A.J.*, 106, 1729
- Fosbury, R. A. E., & Disney, M. J. 1976, *Ap.J. Letters*, 207, L75
- Foschini, L., Ghisellini, G., Tavecchio, F., et al. 2007, *Ap.J. Letters*, 657, L81
- Fossati, G., Maraschi, L., Celotti, A., Comastri, A., & Ghisellini, G. 1998, *MNRAS* , 299, 433
- Fossati, G., Celotti, A., Chiaberge, M., et al. 2000, *Ap.J.* , 541, 166
- Fried, J. W., Stickel, M., & Kühr, H. 1993, *A&A* , 268, 53
- Fujiwara, M., Matsuoka, Y., & Ienaka, N. 2012, *A.J.*, 144, 112
- Gabuzda, D. C., Cawthorne, T. V., Roberts, D. H., & Wardle, J. F. C. 1989, *Ap.J.* , 347, 701
- Gaur, H., Gupta, A. C., Wiita, P. J., et al. 2014, *Ap.J. Letters*, 781, L4
- Ghisellini, G., Maraschi, L., & Treves, A. 1985, *A&A* , 146, 204
- Ghisellini, G., Padovani, P., Celotti, A., & Maraschi, L. 1993, *Ap.J.* , 407, 65

- Ghisellini, G., Villata, M., Raiteri, C. M., et al. 1997, *A&A* , 327, 61
- Ghisellini, G., Celotti, A., Fossati, G., Maraschi, L., & Comastri, A. 1998, *MNRAS* , 301, 451
- Ghisellini, G., & Tavecchio, F. 2008, *MNRAS* , 387, 1669
- Ghisellini, G., Tavecchio, F., Foschini, L., et al. 2010, *MNRAS* , 402, 497
- Ghisellini, G. 2013, *Lecture Notes in Physics*, Berlin Springer Verlag, 873,
- Gioia, I. M., Maccacaro, T., Schild, R. E., et al. 1990, *Ap.J. Suppl.*, 72, 567
- Giommi, P., Menna, M. T., & Padovani, P. 1999, *MNRAS* , 310, 465
- Giommi, P., Piranomonte, S., Perri, M., & Padovani, P. 2005, *A&A* , 434, 385
- Giovannini, G., Falomo, R., Scarpa, R., Treves, A., & Urry, C. M. 2004, *Ap.J.* , 613, 747
- Giroletti, M., Giovannini, G., Taylor, G. B., & Falomo, R. 2004, *Ap.J.* , 613, 752
- Gladders, M. D., Abraham, R. G., McHardy, I. M., et al. 1997, *MNRAS* , 284, 27
- Green, R. F., Schmidt, M., & Liebert, J. 1986, *Ap.J. Suppl.*, 61, 305
- Green, J. C., Froning, C. S., Osterman, S., et al. 2012, *Ap.J.* , 744, 60
- Gu, M. F., Lee, C.-U., Pak, S., Yim, H. S., & Fletcher, A. B. 2006, *A&A* , 450, 39
- Guilbert, P. W., Fabian, A. C., & Rees, M. J. 1983, *MNRAS* , 205, 593
- Gupta, A. C., Krichbaum, T. P., Wiita, P. J., et al. 2012, *MNRAS* , 425, 1357
- Hagen-Thorn, V. A., Larionov, V. M., Jorstad, S. G., et al. 2008, *Ap.J.* , 672, 40
- Halpern, J. P., Impey, C. D., Bothun, G. D., et al. 1986, *Ap.J.* , 302, 711
- Hanson, C. G., & Coe, M. J. 1985, *MNRAS* , 217, 831
- Hartman, R. C., Bertsch, D. L., Bloom, S. D., et al. 1999, *Ap.J. Suppl.*, 123, 79
- Heidt, J., Wagner, S. J., & Wilhelm-Erkens, U. 1997, *A&A* , 325, 27
- Heidt, J., & Wagner, S. J. 1998, *A&A* , 329, 853
- Heidt, J., Nilsson, K., Fried, J. W., Takalo, L. O., & Sillanpää, A. 1999, *A&A* , 348, 113
- Heidt, J., & Nilsson, K. 2011, *A&A* , 529, A162
- H.E.S.S. Collaboration, Abramowski, A., Acero, F., et al. 2012, *A&A* , 539, A149
- H.E.S.S. Collaboration, Abramowski, A., Acero, F., et al. 2013, *A&A* , 552, A118
- Hoffmeister, C. 1929, *Astronomische Nachrichten*, 236, 233
- Hoyle, F., Burbidge, G. R., & Sargent, W. L. W. 1966, *Nature*, 209, 751
- Hudec, R., Bašta, M., Pihajoki, P., & Valtonen, M. 2013, *A&A*, 559, A20
- Hutsemékers, D., Borguet, B., Sluse, D., Cabanac, R., & Lamy, H. 2010, *A&A* , 520, L7
- Impey, C. D., & Tapia, S. 1988, *Ap.J.* , 333, 666
- Impey, C. D., Lawrence, C. R., & Tapia, S. 1991, *Ap.J.* , 375, 46
- Impey, C. D., Bychkov, V., Tapia, S., Gnedin, Y., & Pustilnik, S. 2000, *A.J.*, 119, 1542
- Itoh, R., Fukazawa, Y., Chiang, J., et al. 2013, *PASJ*, 65, 18

- Jannuzi, B. T., Yanny, B., & Impey, C. 1997, *Ap.J.* , 491, 146
- Jorstad, S. G., Marscher, A. P., Larionov, V. M., et al. 2010, *Ap.J.* , 715, 362
- Kastendieck, M. A., Ashley, M. C. B., & Horns, D. 2011, *A&A* , 531, A123
- Kato, T., Uemura, M., Ishioka, R., et al. 2004, *PASJ*, 56, 1
- Kellermann, K. I., & Pauliny-Toth, I. I. K. 1969, *Ap.J. Letters*, 155, L71
- Kinman, T. D. 1975, *Ap.J. Letters*, 197, L49
- Kirk, J. G., Rieger, F. M., & Mastichiadis, A. 1998, *A&A* , 333, 452
- Kotilainen, J. K., Falomo, R., & Scarpa, R. 1998, *A&A* , 336, 479
- Kühr, H., Pauliny-Toth, I. I. K., Witzel, A., & Schmidt, J. 1981, *A.J.*, 86, 854
- Lamer, G., Newsam, A. M., & McHardy, I. M. 1999, *MNRAS* , 309, 1085
- Landoni, M., Falomo, R., Treves, A., et al. 2012, *A&A* , 543, A116
- Landoni, M., Falomo, R., Treves, A., et al. 2013, *A.J.*, 145, 114
- Landoni, M., Falomo, R., Treves, A., and Sbarufatti, B., 2014, *A&A*, submitted
- Larionov, V. M., Villata, M., & Raiteri, C. M. 2010, *A&A* , 510, A93
- Larionov, V. M., Jorstad, S. G., Marscher, A. P., et al. 2013, *Ap.J.* , 768, 40
- Laurent-Muehleisen, S. A., Kollgaard, R. I., Moellenbrock, G. A., & Feigelson, E. D. 1993, *A.J.*, 106, 875
- Laurent-Muehleisen, S. A., Kollgaard, R. I., Ciardullo, R., et al. 1998, *Ap.J. Suppl.*, 118, 127
- Laurent-Muehleisen, S. A., Kollgaard, R. I., Feigelson, E. D., Brinkmann, W., & Siebert, J. 1999, *Ap.J.* , 525, 127
- Maccacaro, T., Gioia, I. M., Maccagni, D., & Stocke, J. T. 1984, *Ap.J. Letters*, 284, L23
- Maccacaro, T., Caccianiga, A., della Ceca, A., Wolter, A., & Gioia, I. M. 1998, *Astronomische Nachrichten*, 319, 15
- MacLeod, J. M., & Andrew, B. H. 1968, *Ap. Letters*, 1, 243
- MAGIC Collaboration, Albert, J., Aliu, E., et al. 2008, *Science*, 320, 1752
- Mannheim, K., & Biermann, P. L. 1992, *A&A* , 253, L21
- Mannheim, K. 1998, *Science*, 279, 684
- Maraschi, L., Ghisellini, G., Tanzi, E. G., & Treves, A. 1986, *Ap.J.* , 310, 325
- Maraschi, L., Ghisellini, G., & Celotti, A. 1992, *Ap.J. Letters*, 397, L5
- Maraschi, L., & Rovetti, F. 1994, *Ap.J.* , 436, 79
- Maraschi, L., & Tavecchio, F. 2003, *Ap.J.* , 593, 667
- Marchã, M. J. M., & Caccianiga, A. 2013, *MNRAS* , 430, 2464
- Marscher, A. P., Jorstad, S. G., Mattox, J. R., & Wehrle, A. E. 2002, *Ap.J.* , 577, 85
- Marscher, A. P., Jorstad, S. G., D’Arcangelo, F. D., et al. 2008, *Nature*, 452, 966
- Maselli, A., Massaro, E., Nesci, R., et al. 2010, *A&A* , 512, A74
- Massaro, E., Giommi, P., Leto, C., et al. 2009, *A&A* , 495, 691
- Massaro, E., Nesci, R., & Piranomonte, S. 2012a, *MNRAS* , 422, 2322
- Massaro, F., D’Abrusco, R., Tosti, G., et al. 2012b, *Ap.J.* , 752, 61
- Massaro, F., Paggi, A., Errando, M., et al. 2013, *Ap.J. Suppl.*, 207, 16
- McBreen, B. 1979, *A&A* , 71, L19

- McHardy, I. M., Koerding, E., Knigge, C., Uttley, P., & Fender, R. P. 2006, *Nature*, 444, 730
- Miller, J. S., & Hawley, S. A. 1977, *Ap.J. Letters*, 212, L47
- Miller, J. S., French, H. B., & Hawley, S. A. 1978a, *BL Lac Objects*, 176
- Miller, J. S., French, H. B., & Hawley, S. A. 1978b, *Ap.J. Letters*, 219, L85
- Miller, H. R., & McGimsey, B. Q. 1978, *Ap.J.* , 220, 19
- Miller, H. R., Carini, M. T., & Goodrich, B. D. 1989, *Nature*, 337, 627
- Moderski, R., Sikora, M., Coppi, P. S., & Aharonian, F. 2005, *MNRAS* , 363, 954
- Moore, R. L., & Stockman, H. S. 1981, *Ap.J.* , 243, 60
- Morris, S. L., Stocke, J. T., Gioia, I. M., et al. 1991, *Ap.J.* , 380, 49
- Mücke, A., & Protheroe, R. J. 2001, *Astroparticle Physics*, 15, 121
- Mücke, A., Protheroe, R. J., Engel, R., Rachen, J. P., & Stanev, T. 2003, *Astroparticle Physics*, 18, 593
- Nesci, R., Tosti, G., Pursimo, T., Ojha, R., & Kadler, M. 2013, *A&A* , 555, A2
- Nicastro, F., Zezas, A., Drake, J., et al. 2002, *Ap.J.* , 573, 157
- Ojha, R., Kadler, M., Böck, M., et al. 2010, *A&A* , 519, A45
- Osone, S. 2006, *Astroparticle Physics*, 26, 209
- Ostorero, L., Villata, M., & Raiteri, C. M. 2004, *A&A* , 419, 913
- Ostriker, J. P., & Vietri, M. 1985, *Nature*, 318, 446
- Ostriker, J. P., & Vietri, M. 1990, *Nature*, 344, 45
- Padovani, P., & Urry, C. M. 1990, *Ap.J.* , 356, 75
- Padovani, P., & Giommi, P. 1995, *Ap.J.* , 444, 567
- Padovani, P., Giommi, P., Landt, H., & Perlman, E. S. 2007, *Ap.J.* , 662, 182
- Padovani, P., Giommi, P., & Rau, A. 2012, *MNRAS* , 422, L48
- Paggi, A., Massaro, F., D’Abrusco, R., Smith, H. A., Masetti, N., Giroletti, M., Tosti, G., & Funk, S. 2013, *Ap.J. Suppl.*, 209, 9
- Paltani, S., & Courvoisier, T. J.-L. 1994, *A&A* , 291, 74
- Pavlidou, V., Angelakis, E., Myserlis, I., et al. 2013, *arXiv:1311.3304*
- Perlman, E. S., Stocke, J. T., Schachter, J. F., et al. 1996, *Ap.J. Suppl.*, 104, 251
- Perri, M., Maselli, A., Giommi, P., et al. 2007, *A&A* , 462, 889
- Persic, M., & de Angelis, A. 2008, *A&A* , 483, 1
- Pesce, J. E., Falomo, R., & Treves, A. 1994, *A.J.*, 107, 494
- Pesce, J. E., Falomo, R., & Treves, A. 1995, *A.J.*, 110, 1554
- Peterson, B. M. 1997, *An introduction to active galactic nuclei*, Cambridge University Press, New York, 1997
- Pian, E., Falomo, R., Scarpa, R., & Treves, A. 1994, *ApJ*, 432, 547
- Pian, E., Urry, C. M., Treves, A., et al. 1997, *Ap.J.* , 486, 784
- Pian, E., Vacanti, G., Tagliaferri, G., et al. 1998, *Ap.J. Letters*, 492, L17
- Pian, E., Romano, P., Treves, A., et al. 2007, *Ap.J.* , 664, 106
- Pietilä, H., Takalo, L. O., Tosti, G., et al. 1999, *A&A* , 345, 760
- Pihajoki, P., Valtonen, M., Zola, S., et al. 2013a, *Ap.J.* , 764, 5
- Pihajoki, P., Valtonen, M., & Ciprini, S. 2013b, *MNRAS* , 434, 3122
- Pirola, V. 1973, *A&A* , 27, 383

- Piner, B. G., Pant, N., & Edwards, P. G. 2010, *Ap.J.* , 723, 1150
- Plotkin, R. M., Anderson, S. F., Hall, P. B., et al. 2008, *A.J.*, 135, 2453
- Plotkin, R. M., Anderson, S. F., Brandt, W. N., et al. 2010, *A.J.*, 139, 390
- Plotkin, R. M., Markoff, S., Trager, S. C., & Anderson, S. F. 2011, *MNRAS* , 413, 805
- Pollock, J. T., Webb, J. R., & Azarnia, G. 2007, *A.J.*, 133, 487
- Potter, W. J., & Cotter, G. 2013, *MNRAS* , 436, 304
- Punch, M., Akerlof, C. W., Cawley, M. F., et al. 1992, *Nature*, 358, 477
- Raiteri, C. M., Villata, M., Capetti, A., et al. 2007, *A&A* , 464, 871
- Raiteri, C. M., Villata, M., Capetti, A., et al. 2009, *A&A* , 507, 769
- Raiteri, C. M., Villata, M., Bruschini, L., et al. 2010, *A&A* , 524, A43
- Raiteri, C. M., Villata, M., D'Ammando, F., et al. 2013, *MNRAS* , 436, 1530
- Rani, B., Krichbaum, T. P., Fuhrmann, L., et al. 2013, *A&A* , 552, A11
- Rector, T. A., Stocke, J. T., Perlman, E. S., Morris, S. L., & Gioia, I. M. 2000, *A.J.*, 120, 1626
- Rector, T.A., & Stocke, J.T. 2003, *AJ*, 125, 2447
- Rieger, F. M. 2004, *Ap.J. Letters*, 615, L5
- Romanishin, W. 1987, *Ap.J.* , 320, 586
- Salpeter, E. E. 1964, *Ap.J.* , 140, 796
- Sambruna, R. M., Maraschi, L., & Urry, C. M. 1996, *Ap.J.* , 463, 444
- Sambruna, R. M., Donato, D., Tavecchio, F., et al. 2007, *Ap.J.* , 670, 74
- Sandrinelli, A., Treves, A., Falomo, R. Farina, E.P., Foschini, L., Landoni, M., & Sbarufatti, B. 2013, *A.J.*, 146, 163
- Sandrinelli, A., Covino, S., & Treves, A. 2014, *A&A* , 562, A79
- Sasada, M., Uemura, M., Arai, A., et al. 2008, *PASJ*, 60, L37
- Sbarrato, T., Ghisellini, G., Nardini, M., et al. 2013, *MNRAS* , 433, 2182
- Sbarufatti, B., Treves, A., & Falomo, R. 2005, *Ap.J.* , 635, 173
- Sbarufatti, B., Falomo, R., Treves, A., & Kotilainen, J. 2006a, *A&A* , 457, 35
- Sbarufatti, B., Treves, A., Falomo, R., et al. 2006b, *A.J.*, 132, 1
- Scarpa, R., & Falomo, R. 1997, *A&A* , 325, 109
- Scarpa, R., Urry, C.M., Falomo, R., & Treves, A. 1999, *ApJ*, 526, 643
- Scarpa, R., Urry, C. M., Falomo, R., Pesce, J. E., & Treves, A. 2000, *Ap.J.* , 532, 740
- Schmidt, M. 1963, *Nature*, 197, 1040
- Schmitt, J. L. 1968, *Nature*, 218, 663
- Schwartz, D. A., & Ku, W. H.-M. 1983, *Ap.J.* , 266, 459
- Schwartz, D. A., Marshall, H. L., Lovell, J. E. J., et al. 2000, *Ap.J. Letters*, 540, L69
- Şentürk, G. D., Errando, M., Böttcher, M., & Mukherjee, R. 2013, *Ap.J.* , 764, 119
- Shakura, N. I., & Sunyaev, R. A. 1973, *A&A* , 24, 337
- Shaw, M. S., Romani, R. W., Cotter, G., et al. 2013, *Ap.J.* , 764, 135
- Shen, Y., Richards, G. T., Strauss, M. A., et al. 2011, *Ap.J. Suppl.*, 194, 45
- Sikora, M., Begelman, M. C., & Rees, M. J. 1994, *Ap.J.* , 421, 153
- Sillanpää, A., Haarala, S., & Korhonen, T. 1988a, *A&A Suppl.*, 72, 347

- Sillanpää, A., Haarala, S., Valtonen, M. J., Sundelius, B., & Byrd, G. G. 1988b, *Ap.J.* , 325, 628
- Sillanpää, A., Takalo, L. O., Pursimo, T., et al. 1996, *A&A* , 305, L17
- Smith, P. S., Allen, R. G., & Angel, J. R. P. 1993, *Ap.J. Letters*, 415, L83
- Smith, E. P., O’Dea, C. P., & Baum, S. A. 1995, *Ap.J.* , 441, 113
- Smith, P. S., Williams, G. G., Schmidt, G. D., Diamond-Stanic, A. M., & Means, D. L. 2007, *Ap.J.* , 663, 118
- Sorcia, M., Benítez, E., Hiriart, D., et al. 2013, *Ap.J. Suppl.*, 206, 11
- Stalin, C. S., Gopal-Krishna, Sagar, R., et al. 2006, *MNRAS* , 366, 1337
- Stein, W. A., Odell, S. L., & Strittmatter, P. A. 1976, *Ann.Rev.A.A.*, 14, 173
- Stickel, M., Padovani, P., Urry, C. M., Fried, J. W., & Kühn, H. 1991, *Ap.J.* , 374, 431
- Stickel, M., Fried, J. W., & Kühn, H. 1993, *A&A Suppl.*, 98, 393
- Stocke, J. T., Morris, S. L., Gioia, I., et al. 1990, *Ap.J.* , 348, 141
- Stocke, J. T., Wurtz, R., Wang, Q., Elston, R., & Jannuzi, B. T. 1992, *Ap.J. Letters*, 400, L17
- Strittmatter, P. A., Serkowski, K., Carswell, R., et al. 1972, *Ap.J. Letters*, 175, L7
- Takahashi, T., Tashiro, M., Madejski, G., et al. 1996, *Ap.J. Letters*, 470, L89
- Takalo, L. O., Sillanpää, A., Nilsson, K., et al. 1992, *A&A Suppl.*, 94, 37
- Takalo, L. O., & Sillanpää, A. 1993, *Ap&SS*, 206, 191
- Takalo, L. O. 1994, *Vistas in Astronomy*, 38, 77
- Tavecchio, F., Maraschi, L., Sambruna, R. M., & Urry, C. M. 2000, *Ap.J. Letters*, 544, L23
- Tommasi, L., Palazzi, E., Pian, E., et al. 2001a, *A&A* , 376, 51
- Tommasi, L., Díaz, R., Palazzi, E., et al. 2001b, *Ap.J. Suppl.*, 132, 73
- Tosti, G., Pascolini, S., & Fiorucci, M. 1996, *PASP*, 108, 706
- Tosti, G., Fiorucci, M., Luciani, M., et al. 1998, *A&A* , 339, 41
- Tosti, G., Massaro, E., Nesci, R., et al. 2002, *A&A* , 395, 11
- Tramacere, A., Giommi, P., Massaro, E., et al. 2007, *A&A* , 467, 501
- Treves, A., Falomo, R., & Uslenghi, M. 2007, *A&A* , 473, L17
- Trussoni, E., Capetti, A., Celotti, A., Chiaberge, M., & Feretti, L. 2003, *A&A* , 403, 889
- Ulrich, M.-H. 1978, *Ap.J. Letters*, 222, L3
- Ulrich, M. H., Hackney, K. R. H., Hackney, R. L., & Kondo, Y. 1984, *Ap.J.* , 276, 466
- Ulrich, M. H. 1989, *BL Lac Objects*, 334, 45
- Ulvestad, J. S., & Antonucci, R. R. J. 1986, *A.J.*, 92, 6
- Urry, C. M., & Shafer, R. A. 1984, *Ap.J.* , 280, 569
- Urry, C. M., & Padovani, P. 1991, *Ap.J.* , 371, 60
- Urry, C. M., Maraschi, L., Edelson, R., et al. 1993, *Ap.J.* , 411, 614
- Urry, C. M., & Padovani, P. 1995, *PASP*, 107, 803
- Urry, C. M., Treves, A., Maraschi, L., et al. 1997, *Ap.J.* , 486, 799
- Urry, C. M., Falomo, R., Scarpa, R., et al. 1999, *Ap.J.* , 512, 88
- Urry, C. M., Scarpa, R., O’Dowd, M., et al. 2000, *Ap.J.* , 532, 816
- Valtonen, M. J., Lehto, H. J., Nilsson, K., et al. 2008, *Nature*, 452, 851

- Vercellone, S., Striani, E., Vittorini, V., et al. 2011, *Ap.J. Letters*, 736, L38
- Vermeulen, R.C., Ogle, P.M., Tran, H.D., Browne, I.W.A., Cohen, M.H., Readhead, A.C.S., Taylor, G.B., Goodrich, R.W. 1995, *ApJ*, 452, L5
- Véron, P., & Véron, M. P. 1976, *A&A* , 47, 319
- Véron-Cetty, M.-P., & Véron, P. 2010, *A&A* , 518, A10
- Villata, M., Raiteri, C. M., Kurtanidze, O. M., et al. 2002, *A&A* , 390, 407
- Villata, M., Raiteri, C. M., Kurtanidze, O. M., et al. 2004a, *A&A* , 421, 103
- Villata, M., Raiteri, C. M., Aller, H. D., et al. 2004b, *A&A* , 424, 497
- Visvanathan, N., & Griersmith, D. 1977, *Ap.J.* , 215, 759
- Visvanathan, N., & Wills, B. J. 1998, *A.J.*, 116, 2119
- Voges, W., Aschenbach, B., Boller, T., et al. 1999, *A&A* , 349, 389
- Wagner, S. J., & Witzel, A. 1995, *Ann.Rev.A.A.*, 33, 163
- Watson, D., Hanlon, L., McBreen, B., et al. 1999, *A&A* , 345, 414
- Weistrop, D. 1973, *Nature*, 241, 157
- Weistrop, D., Smith, B. A., & Reitsema, H. J. 1979, *Ap.J.* , 233, 504
- Weistrop, D., Reitsema, H. J., Smith, B. A., & Shaffer, D. B. 1983, *Ap.J.* , 271, 471
- Westerlund, B. E., Wlerick, G., & Garnier, R. 1982, *A&A* , 105, 284
- Westfold, K. C. 1959, *Ap.J.* , 130, 241
- Wolter, A., Comastri, A., Ghisellini, G., et al. 1998, *A&A* , 335, 899
- Woltjer, L. 1966, *Ap.J.* , 146, 597
- Woo, J.-H., & Urry, C. M. 2002, *Ap.J.* , 579, 530
- Wright, S. C., McHardy, I. M., Abraham, R. G., & Crawford, C. S. 1998, *MNRAS* , 296, 961
- Wurtz, R., Ellingson, E., Stocke, J. T., & Yee, H. K. C. 1993, *A.J.*, 106, 869
- Wurtz, R., Stocke, J. T., & Yee, H. K. C. 1996, *Ap.J. Suppl.*, 103, 109
- Wurtz, R., Stocke, J. T., Ellingson, E., & Yee, H. K. C. 1997, *Ap.J.* , 480, 547
- Zel'dovich, Y. B. 1964, *Soviet Physics Doklady*, 9, 195
- Zhang, X., Zheng, Y. G., Zhang, H. J., et al. 2008, *A.J.*, 136, 1846
- Zhang, B.-K., Wang, S., Zhao, X.-Y., Dai, B.-Z., & Zha, M. 2013a, *MNRAS* , 428, 3630
- Zhang, Y.-H., Bian, F.-Y., Li, J.-Z., & Shang, R.-C. 2013b, *MNRAS* , 432, 1189
- Zhang, H., Chen, X., & Boettcher, M. 2014, *arXiv:1401.7138*